EUROPEAN COMMISSION

HORIZON 2020 PROGRAMME
FUEL CELLS AND HYDROGEN JOINT UNDERTAKING (FCH 2 JU)
TOPIC H2020-JTI-FCH-2015-1
Improved electrolysis for distributed hydrogen production

GA No. 700008

High Performance PEM Electrolyser for Cost-effective Grid Balancing Applications

HPEM$_2$GAS

HPEM2GAS - Deliverable report

D 3.4 Publishable report on catalyst development

Deliverable No.	HPEM2GAS D3.4	
Related WP	WP3- PEM electrolysis components, optimization and scaling-up	
Deliverable Title	**Publishable report on catalyst development**	
Deliverable Date	2018-03-31	
Deliverable Type	REPORT	
Dissemination level	Public (PU)	
Author(s)	A. S. Aricò, S. Siracusano, N. Briguglio, G. Monforte, S. Trocino, C. Lo Vecchio, M.G. Bottari, M. Girolamo, M. Minutoli, V. Baglio (CNR-ITAE) L. Merlo, S. Tonella, C. Oldani (Solvay)	2018-03-05
Checked by	n/a	
Reviewed by (if applicable)	Daniel Greenhalgh (ITM)	2018-03-12
Approved by	Antonino Aricò (CNR-ITAE) - Coordinator	2018-03-20
Status	Final draft	2018-03-22

Disclaimer/ Acknowledgment

This project has received funding from the European Union's Horizon 2020 research and innovation programme under grant agreement No 700008. This Joint Undertaking receives support from the European Union's Horizon 2020 research and innovation programme and Hydrogen Europe, and Hydrogen Europe Research.

Summary

Water electrolysis is a very promising technology for sustainable hydrogen generation using renewable electrical energy. The excellent performance and dynamic behaviour for storing electrical energy in hydrogen allow polymer electrolyte membrane (PEM) electrolysis to cover the gap between the intermittent renewable power production and the grid demand at different time horizons and scales. This deliverable is mainly addressed to the development and characterization of high performance nanostructured Ir-Ru-oxide electro-catalyst achieving for the rate determining oxygen evolution reaction a current density of 3 A cm^{-2} at about 1.8 V (>80% enthalpy efficiency) with a low catalyst loading (0.34 mg cm^{-2}). The stability characteristics were studied in practical PEM electrolysis cells operating at 80 °C, using several durability tests of 1000 h each to evaluate the reliability of this electro-catalyst for real-life operation. Further insights on the degradation mechanism were acquired by subjecting the catalyst to potential steps in a specially designed electrochemical flow cell under corrosive liquid electrolyte with on-line monitoring of the dissolved ions. Structural, morphology, composition and surface analysis of the anode electro-catalyst after operation in the electrolysis cell, complemented by in-situ electrochemical diagnostics, provided important insights into the degradation mechanisms. Catalyst operation at high turnover frequency was observed to cause a progressive change of Lewis acidity characteristics with time for both Ir and Ru cations thus influencing their ability to promote water oxidation.

Nanosized Ir-black (3 nm) and Ir-oxide (5 nm) oxygen evolution electrocatalysts showing high performance in polymer electrolyte membrane (PEM) water electrolysis based on Aquivion® short-side chain ionomer membrane were, also, investigated to understand the role of the Ir oxidation state on the electrocatalytic activity and stability. Despite the smaller mean crystallite size, the Ir-black electrocatalyst shows significantly lower initial performance than the Ir-oxide. During operation at high current density, the Ir-black shows a decrease of cell potential with time whereas the Ir-oxide catalyst shows increasing cell potential resulting in a degradation rate of about 10 µV/h, approaching 1000 h. The unusual behaviour of the Ir-black results from the oxidation of metallic Ir to IrOx . The Ir-oxide catalyst shows instead a hydrated structure on the surface and a negative shift of about 0.5 eV for the Ir 4f binding energy after 1000 h electrolysis operation. This corresponds to the formation of a sub-stoichiometric Ir-oxide on the surface. These results indicate that a hydrated IrO_2 with high oxidation state on the surface is favourable in decreasing the oxygen evolution overpotential. Modifications of the Ir chemical oxidation state during operation can affect significantly the catalytic activity and durability of the electrolysis system.

Contents

1 Introduction

Hydrogen is widely considered a promising energy vector that can act as a mediator between renewable sources and sustainable mobility. As an alternative fuel, hydrogen is characterized by proper energy density and clean combustion. Its wide spread use will assume in the future an increased environmental and societal relevance to address energy issues, pollution, global warming and related climate change effects. Water electrolysis systems connected to renewable power sources represent a reliable process for an efficient and sustainable hydrogen production to power next generation fuel cell vehicles. Among the various water electrolysis technologies, proton conducting polymer electrolyte membrane systems possess the ability to rapidly follow the intermittent energy production from renewable power sources and provide excellent grid-balancing service characteristics to mitigate the differences in energy generation and consumption.

However, PEM electrolysis devices make use of noble metal catalysts, such as Ir, Ru and Pt to work at elevated current densities and to operate durably at high potentials in a protonic environment. The impact of the noble metal catalysts on the cost of PEM electrolysis systems is relevant although these materials are employed with a high level of utilization in electrochemical systems thanks to their nanostructured properties. In principle, the use of noble metal catalysts allows the PEM electrolysis system to operate at high current density (>1 A cm^{-2}) with a corresponding reduction of the electrolyzer capital costs. However, due to the limited availability of noble metal catalysts, a useful strategy is to maximize their utilization in the electrolysis process while operating the electrolysis system at high hydrogen production rates. However, this high current density operation increases both cell potential and temperature thus causing significant durability issues. Commercial PEM electrolysis systems operate at temperatures below 60 °C in order to combine good durability and proper operation of the balance of plant.

However, beside the durability issues, operation at high current density also causes relevant heat management issues. Accordingly, almost all of the state-of-the art PEM electrolysis systems are still operated at current densities of 1 A cm^{-2} or less. The upper temperature limit for operating the present electrolysis cells is about 80 °C. This is essentially determined by the available perfluorosulfonic membranes, e.g. Nafion®. Thus, providing that the balance of plant characteristics and stability of the membrane-electrode assembly (MEA) are improved for high temperature operation, increasing the system operating temperature would result in larger current density and lower overpotentials as result of the accelerated reaction kinetics.

Generally, the degradation of electrolysis systems is affected by pH, electrode potential and temperature effects whereas the components that are mainly subjected to degradation are the anode electrocatalysts (operating at high potentials), bipolar plates and membrane. In particular, the anodic oxygen evolution reaction, is the rate determining step of the entire process and it affects significantly the system stability. An efficient and durable anode operation is a pre-requisite for achieving suitable life-span for the PEM electrolysis systems. This has been recently targeted at 100,000 h. Whereas, to minimize the noble metal catalyst loading, the use of nanosized catalysts with very high surface area is highly desirable. These are however intrinsically less stable than bulk metals or oxides. On the other hand, improving reaction kinetics will imply operation at lower overpotentials for the same hydrogen production rate (making the operating potential window of the electrolysis system smaller) with beneficial effects on the stability.

Most of the efficiency losses occur at the oxygen evolution electrode as this process the rate determining step. Iridium or ruthenium oxides are currently used as oxygen evolution catalysts; they combine proper activity with good corrosion resistance and suitable electronic conductivity. Ruthenium oxides are characterized by higher activity but lower stability than IrO_2. Combining ruthenium and iridium oxides represents a suitable approach to get a trade-off between stability and activity. A very promising method is to form a solid solution by high temperature annealing in order to improve the stability of Ru-oxide while taking advantage of the electronic effects on RuOx on Ir-oxide. However, the high temperature treatment causes a growth of the oxide particles, with a decrease of surface area. Another interesting route is to produce a segregation of the most stable oxide on the surface of the catalyst particles with the least stable phase concentrated in the bulk. This core-shell structure is pursued in many applications, including fuel cells, to (i) get advantage of the electronic effects of the solid solution while avoiding exposing to the electrolyte less stable elements on the catalyst surface and also to (ii) increase electrochemical active surface area (ECSA). Corrosion could be initiated by the presence of an unstable phase on the surface and propagate inside the nanoparticle compromising the stability of the catalytic system.

The purpose of this Deliverable is to provide a structural, composition, surface, and morphology characterization of a solid solution Ir-Ru oxide catalyst with enriched Ir-oxide content on the surface and to study its degradation properties under electrolysis operation at high current densities. The stability characteristics were studied in practical PEM electrolysis cells operating at 80 °C, using several durability tests of 1000 h each and low noble metal loading electrocatalysts to evaluate the reliability of these catalysts for real-life operation. Only a few studies have dealt with the analysis of durability of PEM electrolysis systems using low electrocatalyst loadings and these have essentially regarded monometallic IrO_2 and RuO_2 electro-catalysts. A systematic study on the stability of the Ir-Ru catalyst used at low loading is strongly necessary both in terms of electrochemical and physicochemical analysis. To get more insights on the degradation mechanism, this was exacerbated by subjecting the catalyst to potential steps in a specially designed electrochemical flow cell under corrosive liquid electrolyte with on-line monitoring of the dissolved ions through inductively coupled plasma mass spectrometry (ICP-MS).

Structural, morphology, composition and surface analysis of the electrolysis cell components, complemented by in-situ electrochemical diagnostics provided important insights into the degradation mechanisms. In this Deliverable, we show that dissolution of active species in the Ir-Ru oxide solution occurs according to their surface occurrence rather than the intrinsic stability of the single phases. Thus, the surface segregation offers an appropriate route to stabilize oxygen evolution electrocatalysts while combining advantages in terms of electronic effects to promote electrocatalytic activity.

Recently, significant emphasis has been addressed to the modulation of the Ir oxidation state in the anode catalyst by chemical and electrochemical methods in order to prepare catalysts with enhanced surface roughness corresponding to an increased electrochemically active surface area and improved electrocatalytic activity. However, this argument is still object of debate since other scientific reports have shown that partial reduction of Ir or Ru oxide to form a sub-stoichiometric phase does not appear to bring positive effects.

To provide an additional contribution to the level of knowledge in this field, we have also prepared high surface area metallic Ir and Ir-oxide catalysts with essentially similar primary particle size and evaluated their performance during operation in the PEM electrolysis environment where

formation of a sub-stoichiometric Ir-oxide phase on the surface occurs in both cases. A highly performing short-side chain perfluorosulfonic Aquivion® membrane and ionomer dispersion, specifically designed for water electrolysis, were used to reduce the ohmic resistance thus allowing to investigating the catalyst behaviour at suitable current density with high voltage efficiency. Aquivion® is characterized by both larger crystallinity and higher glass transition temperature than Nafion® with consequent reduction of gas cross-over and improvement of the thermal stability, respectively. It was observed that the oxidation state of the anode catalyst affects significantly the performance and efficiency as well as the stability of the electrolyser. Under galvanostatic operation, the catalyst properties may cause a positive or negative cell voltage variation with time resulting in a specific degradation rate or efficiency improvement, respectively. This seems to depend if the catalyst surface transforms into a more or less active phase. Such evidence requires reconsidering how the impact of the catalyst behaviour on the durability of a PEM electrolysis system is assessed. It appears evident that electrocatalysts showing higher degradation rate but operating at a much better efficiency than other catalytic systems may indeed provide better results during the life span of the electrolysis system.

2 High performance nanostructured catalyst for sustainable water electrolysis

Water electrolysis is a very promising technology for sustainable hydrogen generation using renewable electrical energy. The excellent performance and dynamic behavior for storing electrical energy in hydrogen allows polymer electrolyte membrane (PEM) electrolysis to cover the gap between the intermittent renewable power production and the grid demand at different time horizons and scales. This activity is addressed to the development and characterization of high performance nanostructured Ir-Ru-oxide electro-catalyst achieving for the rate determining oxygen evolution reaction a current density of 3 A cm^{-2} at about 1.8 V (>80% enthalpy efficiency) with a low catalyst loading (0.34 mg cm^{-2}). The stability characteristics were studied in practical PEM electrolysis cells operating at 80 °C, using several durability tests of 1000 h each to evaluate the reliability of this electro-catalyst for real-life operation. Further insights on the degradation mechanism were acquired by subjecting the catalyst to potential steps in a specially designed electrochemical flow cell under corrosive liquid electrolyte with on-line monitoring of the dissolved ions. Structural, morphology, composition and surface analysis of the anode electro-catalyst after operation in the electrolysis cell, complemented by in-situ electrochemical diagnostics, provided important insights into the degradation mechanisms. Catalyst operation at high turnover frequency was observed to cause a progressive change of Lewis acidity characteristics with time for both Ir and Ru cations thus influencing their ability to promote water oxidation.

2.1 Materials and methods for IrRuOx catalysts

A nanosized IrRu-oxide electro-catalyst was prepared using the Adams method according to the procedure reported in D3.1; in the present case, the final thermal treatment (500 °C for 10 min) was optimized to achieve a good compromise between average crystallite size smaller than 10 nm while improving crystallographic properties. A leaching in perchloric acid 0.1 M for 1 h at 80 °C followed by extensive washing was carried out. A sulphite complex procedure (D3.1) was used for preparing a 30% Pt/C cathode catalyst. A 90 μm polymer electrolyte extruded membrane from Solvay Specialty Polymers based on a chemical stabilized Aquivion® SSC ionomer (E98-09S) with 1000 g/eq equivalent weight (EW) was used [32]. The catalyst-coated membrane was prepared by spray-coating using a catalyst ink, containing $Ir_{0.7}Ru_{0.3}Ox$ at the anode and Pt/C at the cathode in combination with an Aquivion® D83-06A dispersion (Solvay Specialty Polymers). The CCM was subjected to a hot-pressing procedure at 190°C for 1.5 min under a compressive force of 20 kg·cm^{-2}. A carbon cloth based diffusion layer was used at the cathode as backing layer whereas a titanium fibre mesh (Bekaert Toko Metal Fiber Co.) was used as backing layer for the anode. The MEA was installed in a single cell test fixture with 5 cm^2 active area made of machined titanium plates. Two different catalyst loadings were used for the anode i.e. 0.34 mg Ir+Ru cm^{-2} (referred as low loading) and 1.27 mg Ir+Ru cm^{-2} (referred as high loading) whereas the Pt loading at the cathode was kept constant at 0.1 mg cm^{-2}.

The performance and stability of the electrolysis cells was studied at 80 °C and under ambient pressure using an Autolab PGSTAT 302 Potentiostat/Galvanostat equipped with a 20 A booster (Metrohm) and FRA (frequency response analyzer). Deionized water (Milli-Q Integral, Millipore, 18.2

MΩ·cm) was fed to the anode at 4 mL·min^{-1} and recirculated at the same cell temperature. Chronopotentiometric studies were carried out at constant current density (1 A cm^{-2} or 3 A cm^{-2}) for 1000 h. At the beginning and the end of the chronopotentiometric tests, polarization curves in galvanostatic mode electrochemical impedance spectroscopy (EIS) and cyclic voltammetry (20 mV·s^{-1}) were carried out to serve as in-situ electrochemical diagnostics.

Structural, chemical, surface and morphology ex-situ characterization was carried out on the raw catalysts as well as on both fresh and used (after the 1000 h durability test) electrocatalytic layers.

X-ray diffraction (XRD) was carried out using a Panalytical X-Pert instrument with a CuKa radiation. The diffraction patterns were interpreted using the Joint Committee on Powder Diffraction Standards (JCPDS). The morphology and nanostructure was investigated by scanning transmission electron microscopy (STEM) carried out in a Cs corrected microscope CF-ARM Jeol operated at 200 kV, equipped with a SSD Jeol EDX spectrometer. The specimens were prepared by sample dispersion in alcohol and subsequently depositing a few drops of the suspension on a carbon-coated copper grid. The surface composition of the IrRu oxide-based anodes, before and after the 1000 h time-test, was investigated by using a Physical Electronics (PHI) 5800-01 spectrometer. A monochromatic Al Kα X-ray source was used at a power of 300 W. X-ray photoelectron spectra were obtained with a pass energy of 58.7 eV for elemental analysis. The pressure in the analysis chamber of the spectrometer was 1·10-9 Torr during the measurements. Quantitative analyses were carried out by dividing the integrated peak area by atomic sensitivity factors, which were calculated from the ionization cross-sections, the mean free electron escape depth and the measured transmission functions of the spectrometer. XPS data were interpreted by using the on-line library of oxidation states implemented in the PHI Multipak 6.1 software.

In the setup an electrochemical flow cell is coupled with ICP-MS. In summary, a commercial BASi electrochemical flow cell (Cross-Flow Cell Kit MW-5052) with a homemade silicon gasket of a 1 mm thickness was coupled with an Agilent 7500ce ICP-MS instrument (Agilent Technologies, Palo Alto, USA) equipped with a MicroMist glass concentric nebulizer and a Peltier cooled Scott-type double-pass quartz spray chamber. A forward radio frequency power of 1500 W was used with Ar gas flows: carrier 0.85 L/min, makeup 0.28 L/min, plasma 1 L/min, and cooling 15 L/min. 0.1 mol/L $HClO_4$ (Aldrich 70%, 99.999% trace metals basis) acid was used as the electrolyte carrier medium. Solutions were pumped at 153 µL/min using a syringe pump (WPI sp100i). Catalyst thin film preparation was as follows: catalyst powder was dispersed in Milli-Q water resulting in a concentration of 0.1 mg/mL. Suspension was cast dropped over a gold disk electrode (d = 3mm) and stabilized by a 5 µL of Nafion diluted by isopropanol (1/50). The deposited amount of catalyst was 0.5 µg resulting in a catalyst loading of 7 µg/cm$^2_{geo}$. Experimental procedure was initiated by OCP measurement for 300 s. Afterwards a sequence of: three potential holds at 1.6 V vs RHE each of which lasted for 120 s. In between each of these holds, an OCP measurement was conducted for 120 s. Afterwards three potential holds at 1.8 V for 120 s were performed, in between each, an OCP measurement of 120 s was conducted. After these three potential holds at 1.6 V vs RHE for 120 s were performed, again each of which was interrupted for 120 s of OCP monitoring.

2.2 Results and Discusison on IrRuOx Catalysts

The structural properties of the mixed Ir- and Ru-oxide oxygen evolution catalyst prepared by a modified Adams synthesis followed by a surface leaching treatment in hot acid solution ($HClO_4$, 0.1 M, 80 °C) were investigated by X-ray diffraction. IrO_2 and RuO_2 oxides are characterized by the same rutile structure with very similar lattice parameters; thus, it is difficult to differentiate between separate phases and solid solution. The X-ray pattern in Fig. 1 shows the typical reflections of the tetragonal rutile crystallographic structure of IrO_2 and RuO_2. However, the shift of the diffraction peaks towards higher Bragg angles (e.g. the 211 reflection occurs at 54.40° as shown in the inset of Fig.1 with respect to 54.15° expected for IrO_2) indicates the occurrence of a lattice contraction as consequence of the formation of a solid solution. Moreover, the presence of a single diffraction peak at 66.5° in the region where two reflections, 310 and 112, of similar intensity typical occur in RuO2 or in separate IrO_2 – RuO_2 mixtures is also indicative of the presence of solid solution (Fig.1). A 70:30 at. composition for the solid solution IrO_2:RuO_2 is estimated from the shift of diffraction peaks in accordance with the nominal composition. This composition was selected to obtain complete solubilization of RuO_2 in the IrO_2 lattice while avoiding excess of RuO_2 on the surface that may corrode in acidic environment through oxidation to RuO_4 and subsequent dissolution. The mean crystallite size determined from the Debye-Scherrer equation is about 7.6 nm.

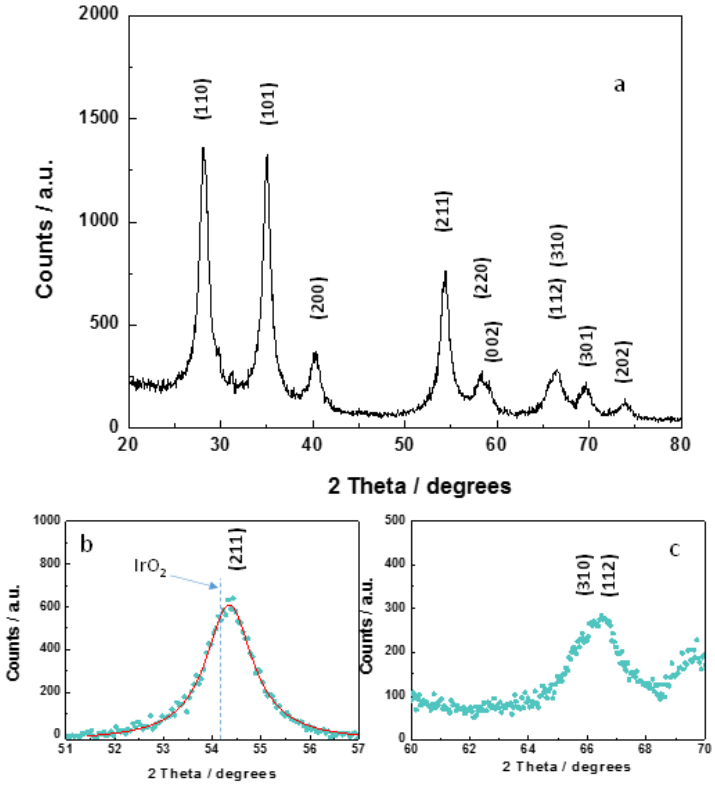

Fig.1a-c X-ray diffraction patterns of the anodic IrRuOx catalyst and high resolution scans of specific two theta regions

The IrRu-oxide catalyst morphology investigated by transmission electron microscopy, showed a mixture with small irregular shape particles and faceted particles (Fig. 2a-b). For what concerns the faceted particles, squared shape nanocrystals (2D-image) were clearly evident together with elongated or rod-like (rectangular shape) particles. Most of the square shape particles were characterized by a dimension smaller than 10-15 nm where a few rod-like particles showed a length up to 25 nm (Fig. 2b). Analysis at higher magnification (see below) showed the occurrence of very small regular nanocrystals together with fine irregular particles (<10 nm). A particle size distribution cannot be easily carried out for this type of morphology and particle shapes. However, it seems that the average crystal size estimated from the broadening of X-ray diffraction provides a good representation of the mean particle size of the material. Electron diffraction (Fig. 2c) essentially confirmed the rutile structure and the polycrystalline nature of this material whereas the broadening of the diffraction rings was indicative of the prevailing occurrence of very fine particles.

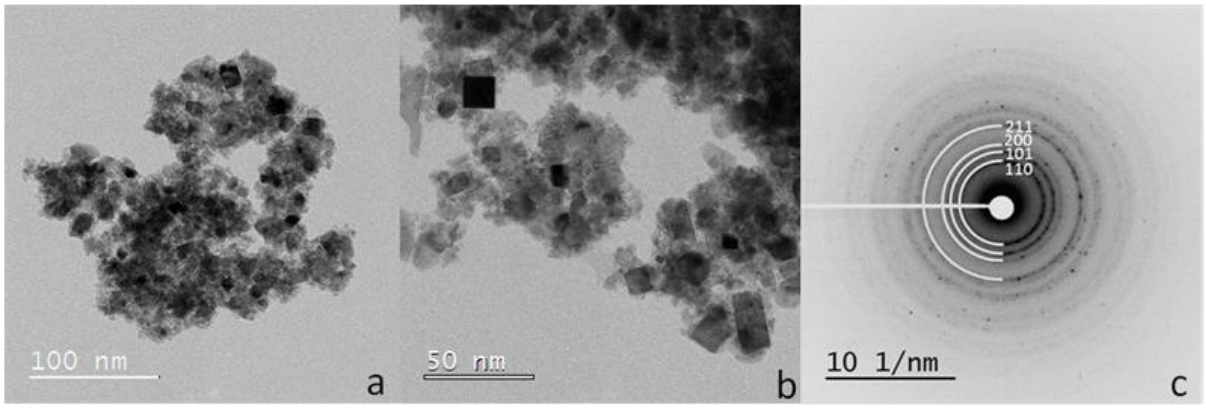

Fig. 2a-c Transmission electron micrographs (a,b) of the anodic IrRuOx catalyst and electron diffraction pattern (c).

High-angle annular dark-field imaging (HAADF) for faceted and irregular shape particles is shown in Fig. 3a. This technique is sensitive to the atomic number of atoms present in the material (Z-contrast). Being the atomic number of iridium and ruthenium quite different (Ir=77 and Ru=44), it is possible to make distinctions on the basis of Z-contrast imaging; however, chemical information from EDX is useful to support. It seems that there is a good intermixing between Ir and Ru especially in the particles with irregular shape (Fig. 3b). Squared (2D-image) nanocrystals with dimension as small as 3 nm are also present (Fig. 3a). The nanocrystals with irregular shape are crystalline in nature; most of them show small dimensions e.g. 5 nm. The presence of different crystal orientations is clearly seen in the irregular particles. It is however unclear why some particles have crystallized forming well defined nanocrystals of very low size whereas other particles have kept the irregular shape conformation of the amorphous precursor which is an intermediate phase of this preparation procedure. This may be related to an inhomogeneous heat flow during thermal treatment or a transition state which has not achieved its thermodynamic equilibrium state. We have tailored the temperature and time of the treatment in order to have the optimal trade-off between well crystallized particles while avoiding relevant growth that causes loss of surface area and decrease of the number of sites available for the reaction.

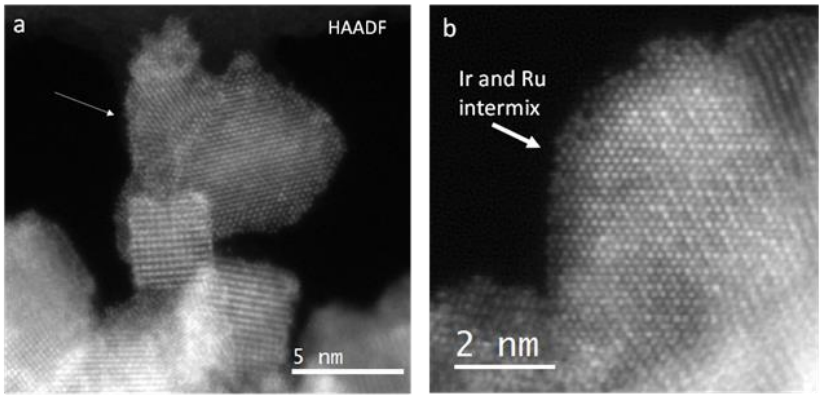

Fig. 3a-b High-angle annular dark-field imaging (HAADF) for faceted and irregular shape particles at two different magnifications for the IrRuOx anode catalyst.

However, it should be pointed out that oxygen evolution is a structure sensitive reaction and the presence of small nanocrystals with well defined orientation (Fig. 4a), most of them show well defined (110) facets, as evident in the reciprocal space (Fig. 4a,b), may play a relevant role for the process. A close analysis at high magnification shows that the regular particles are indeed prevailing (Fig. 5a) even if some of them, being very small in size, may appear irregular at low magnification. It is also clear that elongated particles show defined (110) facets, some of them with very regular shapes and free of defects whereas other particles show the presence of lattice defects and dislocations (Figs. 5b).

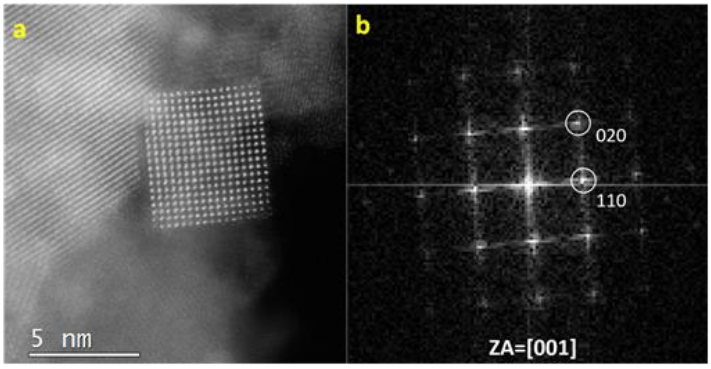

Fig. 4a-b Microstructural properties of the IrRuOx anode catalyst

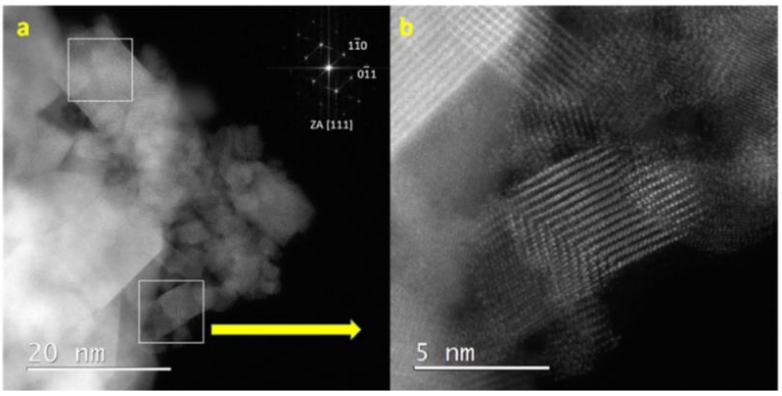

Fig. 5a-b Crystallinity and defects characteristics of fine particles in the IrRuOx catalyst

Beside the microstructural aspects, the surface chemistry of this catalyst is very important in terms of both activity and performance. Scanning transmission electron microscopy (STEM) annular dark field imaging was also performed in parallel to Energy-dispersive X-ray spectroscopy (EDX) mapping (Fig. 6). In principle, the distribution of both Ir and Ru appears homogeneous along the agglomerate (Fig. 6). However, it is noted that the contours (edges) of the agglomerate are more easily reproduced by the Ir M mapping (Fig. 6c) than the Ru mapping (Fig. 6d) as compared to the STEM BF and ADF images. The contours of the agglomerate observed from O K mapping (Fig. 6e) appear more similar to the Ir map even if the Ir M distribution better represents the agglomerate shape. According to this evidence, the surface contours of the agglomerate are mainly composed by Ir atoms whereas it is not exclude that some internal regions are enriched of Ru as it may be seen from the overlay image (Fig. 6f).

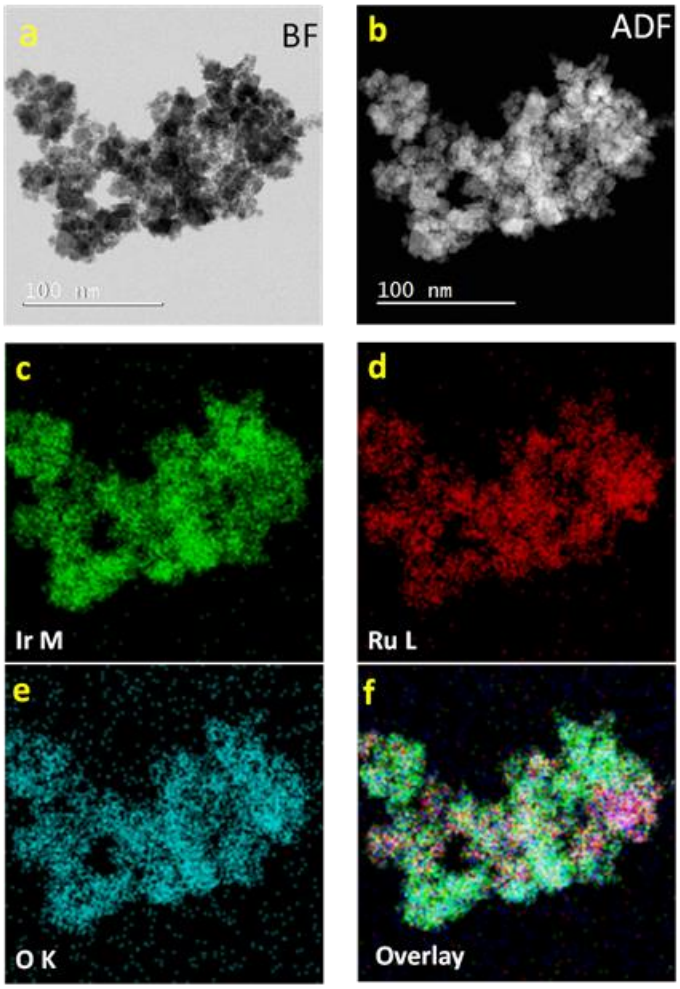

Fig. 6a-f Bright field (a), annular dark field (b) Imaging and EDX mapping (c-f) of the IrRuOx catalyst agglomerate at low magnification.

This evidence was confirmed by doing the same analysis at higher magnification (Fig. 7). In particular, the shape of a large rectangular particle (indicated by an arrow in Figs 7a-f) is well reproduced in terms of contours by the Ir mapping whereas the edges of this particle are less clear in both the Ru and O mapping (Figs 7 d,e). Interestingly, the Ir mapping (Fig. 7c) shows that the core of the rectangular shape

particle is somewhat empty of Ir atoms and the same core regions are enriched with Ru atoms. The overlay image (Fig. 7f) confirms such aspect. This is a clear evidence of an enrichment of the core of faceted particles with Ru atoms whereas their surface is essentially composed of Ir atoms. The fact, that also oxygen atoms are less occurring on the surface would indicate the presence of sub-stoichiometric Ir atoms in the outermost layer. This is also confirmed by XPS analysis of the catalyst powder (see below). Beside the shaped particles also the other regions of the agglomerate show Ru atoms more concentrated in the inner parts where the Ir atoms are prevailing at the contours of the agglomerate (Fig 7). EDX line scan analysis of large rectangular particles (Fig. 8a-b) clearly shows an Ir enrichment close to the edge of the particle whereas Ru is essentially concentrated in the core of the particle. Distribution of oxygen atoms is showing almost constant distribution in the bulk of the particle but decreasing rapidly at the surface where Ir atoms appear prevalent with very likely sub-stoichiometric properties.

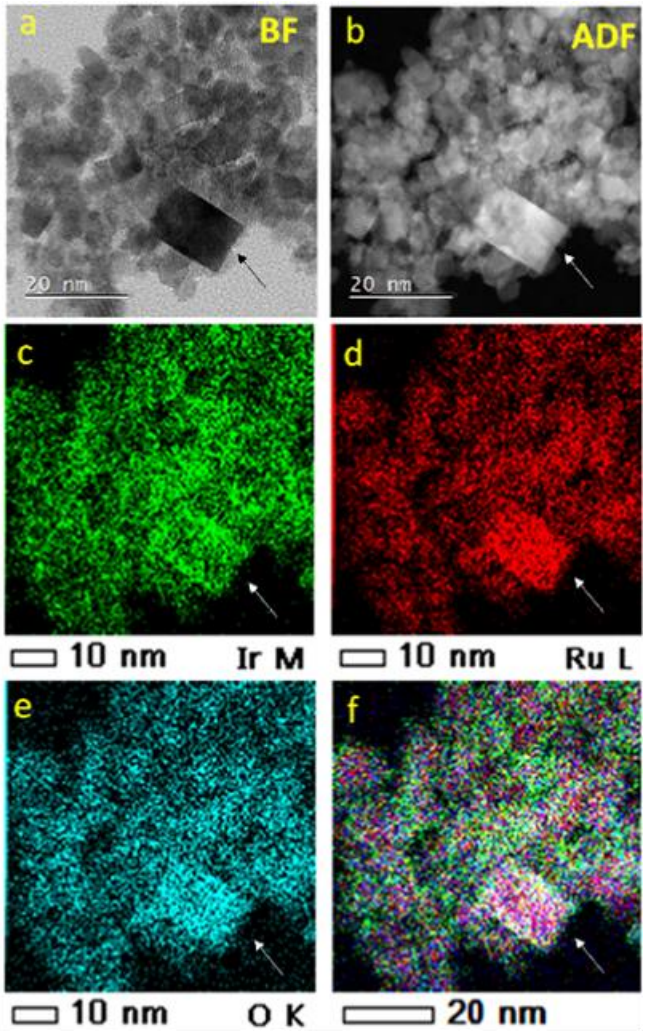

Fig. 7a-f Bright field (a), annular dark field (b) Imaging and EDX mapping (c-f) of the IrRuOx catalyst agglomerate at high magnification.

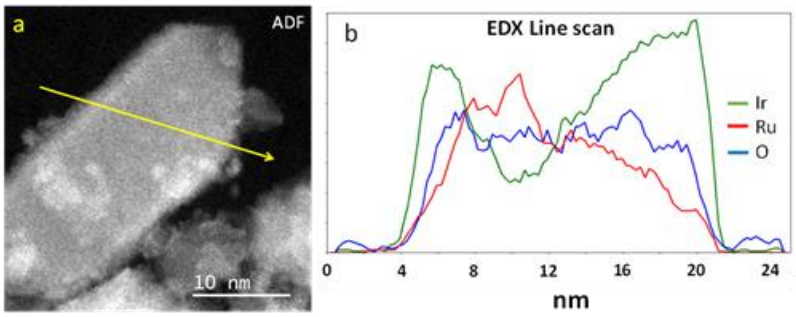

Fig. 8a-b Energy dispersive X-ray analysis (EDX) line scan along an IrRuOx catalyst particle

Although several sample regions where analyzed by TEM and the picture provided above appears representative of the entire sample, it was appropriate to corroborate such evidences by an X-ray electron spectroscopy analysis. The most relevant portion of the XP survey spectrum is shown in Fig. 9 where the main Ir and Ru photoelectron lines are shown. The surface atomic ratio between Ir and Ru was about 3.9 as determined from the Ir 4f and Ru3p3/2 analysis. The Ru3p3/2 was selected for the quantitative analysis since it is not affected by any interference as opposite of the more intense Ru3d peak (see below). The large Ir/Ru ratio indicates some segregation of Ir on the surface. After a sputtering procedure, the Ir/Ru ratio obtained by XPS decreased to 2.3 that is similar to the nominal composition (Ir:Ru 70:30). Regarding the XPS derived composition, it is important to mention that the depth analysis of this technique is around 3 nm; thus, the XPS results deal with the average composition of several outermost layers; however, the results are in agreement with those obtained from electron microscopy.

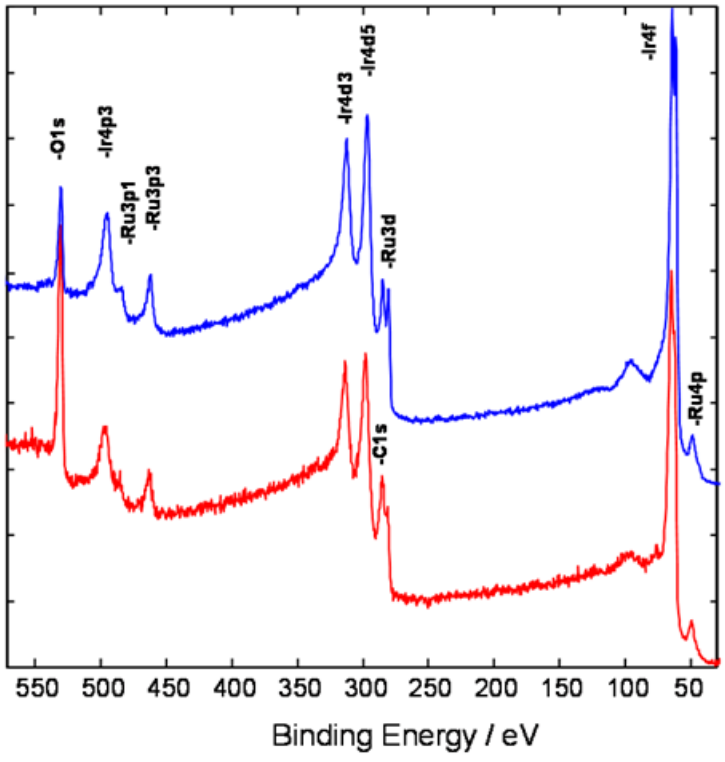

Fig. 9 Survey XP spectrum of the pristine and sputtered IrRuOx catalyst

High resolution XPS analysis of the Ir 4f7/2 peak (Fig. 10) shows its occurrence at 62 eV; deconvolution confirms the prevailing occurrence of sub-stoichiometric Ir3+ (56%) in the outermost layers. This seems to be not the case of Ru. The analytical 3d Ru peak at 281 eV is clearly associated to the Ru4+ oxidation state i.e. in agreement with the even distribution of oxygen inside the particles where Ru is mostly occurring.

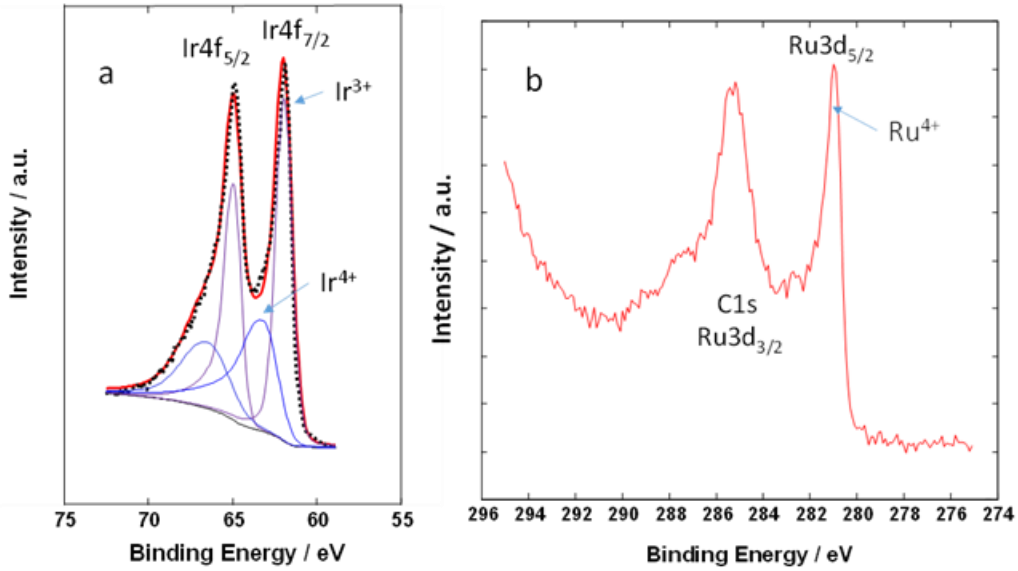

Fig. 10a-b High resolution Ir 4f (a) and C1s-Ru3d (b) XP spectra of the pristine IrRuOx catalyst

As discussed in the Introduction, the oxygen evolution is the rate determining step in a PEM electrolysis process. Accordingly, commonly a high overpotential is necessary to allow the oxygen evolution to occur at high rates. On the other hand, hydrogen evolution on carbon-supported Pt electrodes occurs at high rate with a very low overpotential. In a PEM electrolysis cell, the cathode, where hydrogen evolution reaction occurs, can be treated as counter and reference electrode. Being very little polarized also at high current densities, its potential does not differ significantly from the reversible hydrogen electrode. The membrane has the major impact on the ohmic resistance. Ohmic drop can be relevant at high currents especially in the presence of a thick membrane. This is often selected to avoid hydrogen gas cross-over due to high differential pressure operation used in PEM electrolysis. In the present work, we have selected a 90 µm thick short-side chain perfluorosulfonic acid Aquivion® membrane, characterized by higher crystallinity than conventional Nafion®, lower equivalent weight (EW), i.e. 980 g/eq, and reduced gas cross-over. The ohmic resistance recorded at 80 °C for the PEM electrolysis system under study was about 0.09 Ohm·cm^2. In a relevant working mode, the cathode (hydrogen electrode) is not contributing to the cell degradation since it is being operated at very low potential.

Degradation of PEM electrolysis cells is instead strongly related to the anode catalyst characteristics since the electrode is exposed to high potentials. The variables that are usually considered to drive the corrosion of an electrode material are essentially the operating pH, temperature and potential. In our study, we have kept constant the temperature (80°C) and the protonic (pH) environment, which is determined by the specific membrane and ionomer dispersion used in the composite electrocatalyst layers while we have varied the current load and catalyst loading. In particular, we have selected two

different current densities for each catalyst loading corresponding to different operating cell potentials in a range of practical interest.

In electro-catalytic systems, such as fuel cells and electrolyzers, the degradation rate usually increases when the catalyst loading decreases. This aspect is widely observed experimentally even if a clear understanding of the phenomenon is not yet reached. Here, this aspect is analyzed by considering that a reduction of catalyst loading causes an increase of the turn over frequency or the site time yield (number of evolved oxygen molecules per second on a single catalytic site) when the electrochemical system is operated at the same current density.

The water splitting is an endothermic process, however to occur at significant rates it is necessary to operate the electrolysis system significantly above the thermoneutral potential (1.47 V vs. RHE at 80 °C). Thus, the process becomes exothermic possibly causing hot spots with catalyst sintering and dissolution. Therefore, the catalyst loading is also a relevant parameter. In principle, decrease of catalyst loading may produce a reduction of capital costs (CAPEX) but may also affect negatively the life-span and performance of the electrolysis system and the operating expenditures (OPEX), especially if corrosion is exacerbated.

Membrane-electrode assemblies were prepared with two significantly different Ir-Ru anode catalyst loadings i.e. 0.34 mg·cm^{-2} and 1.27 mg·cm^{-2}. Whereas, the Pt loading at the cathode was 0.1 mg·cm^{-2}. There was no need to use larger Pt loading here since the hydrogen evolution was not a rate determining step. Two durability tests were carried out at 1 A·cm^{-2} and 3 A·cm^{-2}, for each catalyst loading. In total four durability tests of 1000 h were carried out (Fig. 11). It is worth pointing out that operation of the system at 3 A·cm^{-2} means tripling the current density with respect to state of the art electrolysis systems.

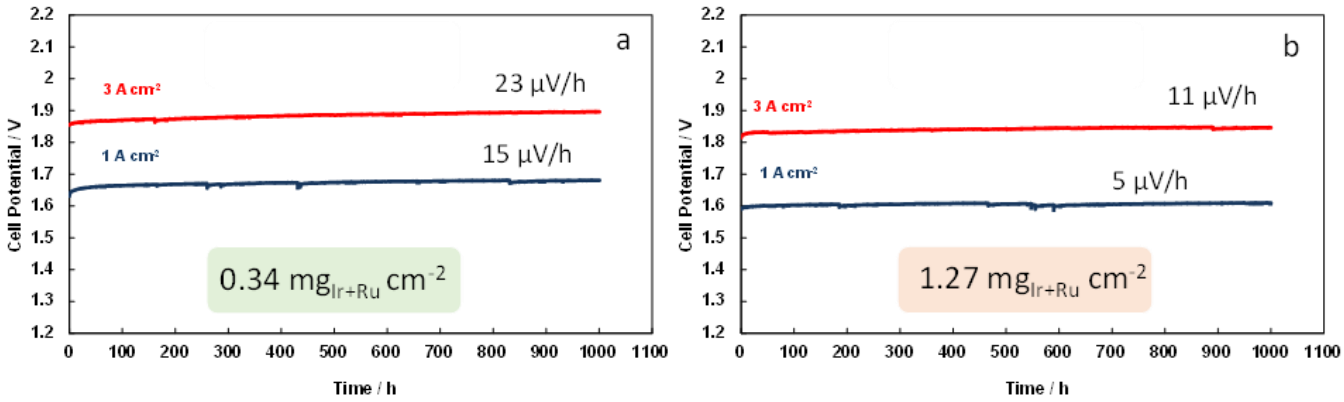

Fig. 11a-b Steady-state durability tests of electrolysis cell at 1 and 3 A·cm^{-2} for low (a) and high (b) catalyst loading MEA configurations

The corresponding initial cell voltages were around 1.6 V and 1.8 V, at low and high currents in the case of the larger catalyst loading (Fig. 11a) corresponding to an enthalpy efficiency of about 90 % and 80 %, respectively. These operating conditions can allow an efficient conversion of renewable energy to hydrogen under different loads as necessary to address the variable energy supply.

The degradation rate in Fig. 11 was estimated from the linear fitting of the voltage increase during the entire test but excluding the first 100 h that can be considered a typical conditioning period where

reversible degradation essentially due to mass transport constraints is prevailing. Whereas a test of 1000 h represents the minimum operating period to make an estimation of the life-time of the electrolysis system.

Fig. 11a shows the cell endurance tests for the MEA with low catalyst loading (0.34 mg cm^{-2}). The cell potentials at the beginning of each experiment for the two operating current densities, 1 A cm^{-2} and 3 A cm^{-2}, were 1.65 V and 1.85 V, respectively. The degradation rate was 15 µV/h at 1 A cm^{-2} and increased to 23 µV/h at 3 A cm^{-2}. Thus, there was a significant effect of the operating current density/cell voltage on performance degradation. The degradation rate increased however less than twice with a three-fold increase of current load.

The same experiment was repeated with another MEA prepared with much larger anode catalyst loading, i.e. 1.27 mg cm^{-2} (Fig. 11b). The cell potentials at the beginning of each experiment for the two operating current densities, 1 A cm^{-2} and 3 A cm^{-2}, were 1.6 V and 1.8 V, respectively. Thus, the operating potential was roughly 50 mV lower than for the previous MEA for each current load condition. The degradation rate was significantly lower for the high catalyst loading MEA i.e. 5 µV/h at 1 A cm^{-2} and increased to only 11 µV/h at 3 A cm^{-2} (Fig. 11b). It is observed that the cell with higher catalyst loading operating at about 1.8 V at 3 A cm^{-2} showed slightly lower degradation rate than the cell with lower catalyst loading operating at 1.65-1.7 V at lower current density (1 A cm^{-2}). Thus, according to these results, the low catalyst loading appears to play a role more relevant than the cell potential in determining the degradation rate (µV/h). Since the catalyst loading was decreased almost four times in these experiments (from 1.27 mg cm^{-2} to 0.34 mg cm^{-2}) the corresponding increase of the corrosion rate appears to be related more to the increase of the turn-over frequency than to the operating potential window. Therefore, the large increase of degradation rate at low catalyst loading under operation at 3 A cm^{-2} is very likely produced by the strong increase of turn-over frequency. A progressive increase of the degradation rate with the turnover frequency, here reported as mass-normalized electrolysis current (A/g), is observed in Fig. 12a. A possible explanation of this phenomenon could be searched into the amount of heat that is released per unit of time and amount of catalyst loading (i.e. per catalytic site) during operation. The electrolysis process is exothermic above the thermoneutral potential; thus, the amount of thermal power produced per unit amount of catalyst loading can be obtained from the following formula:

$$W_{th} = (E_{cell,in}-E_{th}) \cdot I / m_{cat} \; ; \; W_{th} \equiv W \cdot mg^{-1}$$

where W_{th} is the thermal power produced per unit amount of catalyst loading, Ecell is the initial operating cell potential at the specific current density, Eth is the thermoneutral potential (1.47 V at 80 °C), I is the current density, mcat is the catalyst mass loading normalized per electrode geometric area. Fig. 12b shows a relationship between corrosion rate and heat released per unit of time and amount of catalyst. The trend is similar to that observed between degradation rate and turnover frequency in Fig. 12a. Although the limited number of experiments (every test is lasting 1000 h) carried out does not allow definitive considerations, very likely the local heat produced by the electrochemical exothermic process can cause particle sintering, growth, dissolution etc. This justifies the increase of the degradation rate with the increase of current density and the decrease of catalyst mass loading. Whereas, less relevant appears the effect of the operating potential window. Although an increase of corrosion rate with the increase of cell potential is expected, this trend can be masked by the prevailing

role of the increased turn over frequency and the effect of the corresponding heat released during operation.

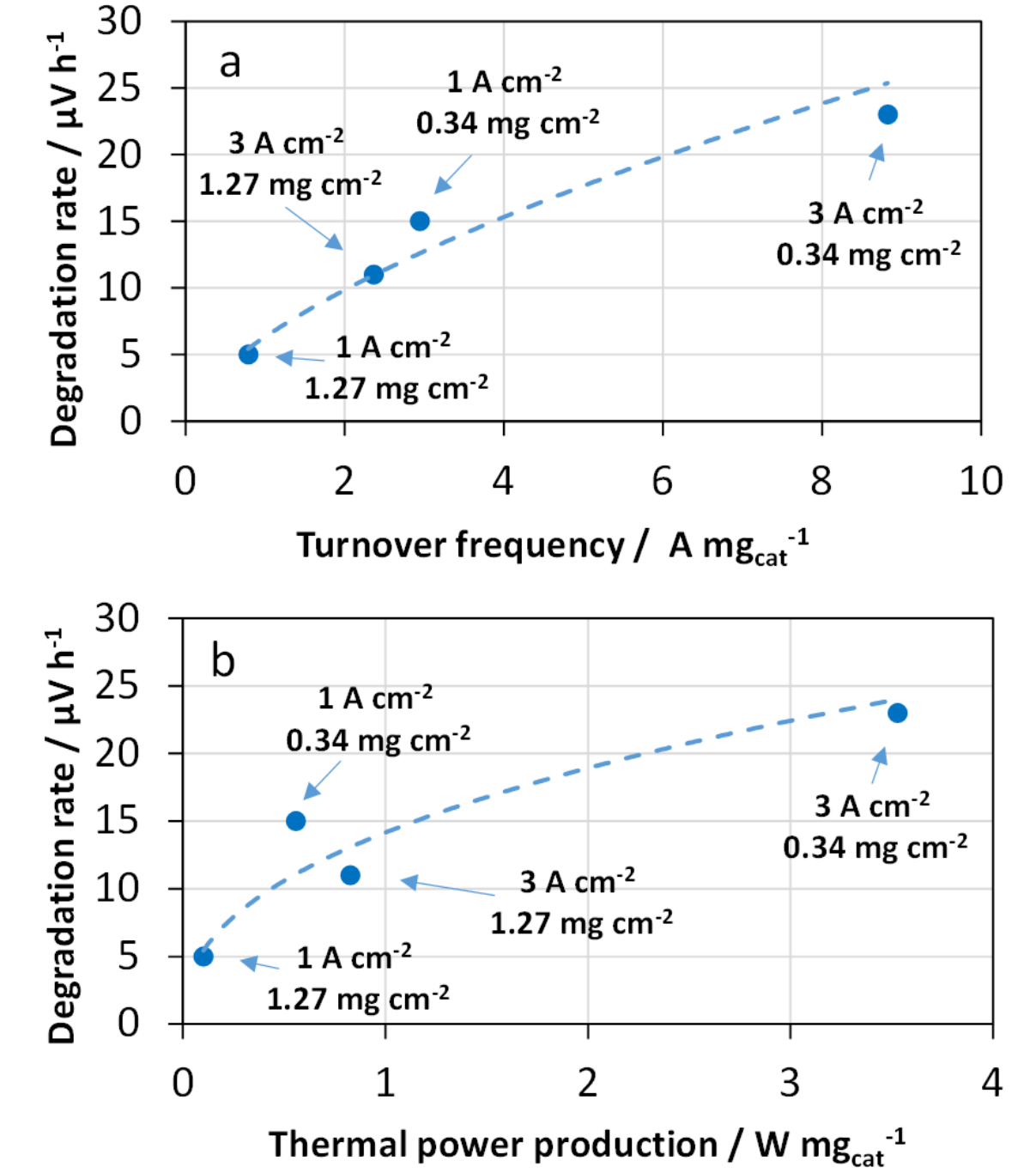

Fig. 12a-b Variation of the degradation rate for electrolysis cells with different anode catalyst loading and operated for 1000 hrs at different current densities as a function of the turn over frequency (a) and thermal power output (b).

The polarization curves for the PEM electrolysis cell clearly show, especially in the case of the low loading MEA (Fig.13), that there is a larger increase of potential (including an increase of the onset

potential) after 1000 h operation at 3 A cm^{-2}. This increase of cell potential corresponds to a loss of efficiency for the water splitting process and it mainly occurs in the activation region at low current density (Fig. 13). Whereas the slope of the curves at high current density (ohmic region) is very similar (there was indeed a decrease of ohmic drop from 0.09 to 0.08 Ohm cm^2 as measured by ac-impedance. Thus, the cell degradation is essentially catalytic in nature. Since no relevant evidence of electrochemical surface area loss was observed (not shown), instead there was a slight increase of coulombic charge for the anode adsorption processes after operation, catalyst modifications may have occurred essentially in terms of roughness and surface chemistry, and possibly not in terms of catalyst sintering.

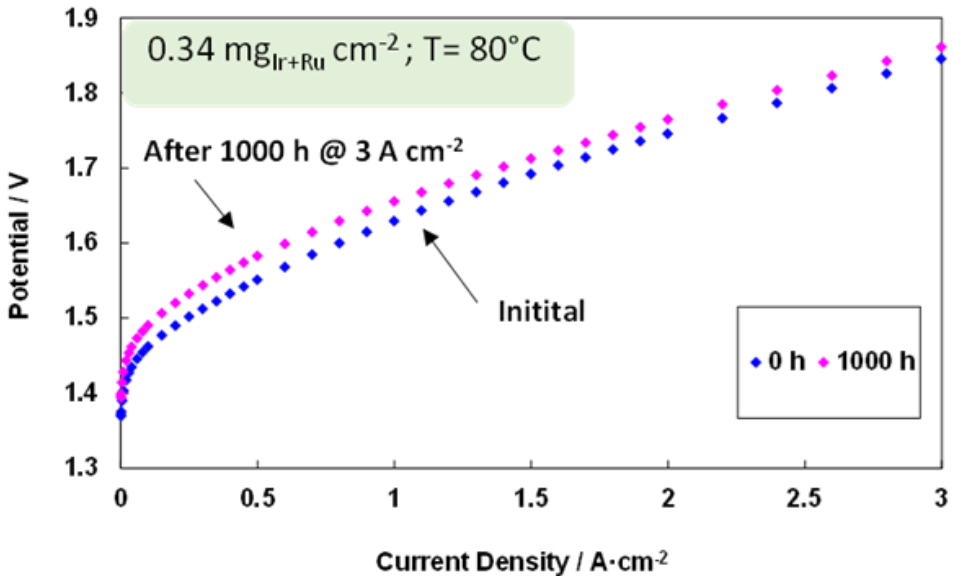

Fig. 13 Electrolysis polarization curves for the low catalyst loading MEA before and after operation at 3 A cm^{-2} for 1000 h at 80 °C.

XPS analysis was carried out on the anodic surface of a fresh MEA and on two MEAs operated for 1000 h at different turn over frequency (Fig. 14a-c). These were a MEA loaded with 1.27 mg cm^{-2} IrRu-oxide and operated at 1 A cm^{-2}, and a MEA loaded with 0.34 mg cm^{-2} and operated at 3 A cm^{-2}. It is anticipated that the presence of the ionomer (ionic polymer) dispersion in the electrocatalyst layer makes difficult to separate the Ru3d from the C1s signal since these occur at very close binding energies (Fig. 14b). Thus, the Ir4f and Ru 3p3/2 photoelectron lines were selected for quantitative analysis of the relative surface concentrations of Ir and Ru. The composition was determined before (B.S.) and after sputtering (A.F.) to get information on surface and bulk characteristics.

XPS analysis of fresh electrode and high catalyst loading anode operated for 1000 h at 1 A cm^{-2} showed similar Ir/Ru ratio (3.8 at.) as in the pristine sample with a clear evidence of surface enrichment in Ir. The atomic Ir/Ru ratio decreased to about 1.8-1.9 after sputtering (Table 1). Interestingly, the surface composition (B.S.) of the low catalyst loading anode operated for 1000 h at 3 A cm^{-2} was not significantly different from its bulk (A.S.) composition differing from the previous electrodes. A possible erosion of the outermost layers in the electrode operated at much higher turnover frequency may explain such evidences; in this regard, the slight increase of coulombic charge associated to the adsorption processes [67,68] in cyclic-voltammograms (Fig. S6) may be due to an increased surface

roughness. The slight difference in surface composition between the catalyst powder and the fresh electrode may be due to the fact that part of the catalyst agglomerates are covered by the perfluorosulfonic acid ionomer micelles causing a variation of the analysis depth for the catalyst as well as modification of the oxidation states (Table 1).

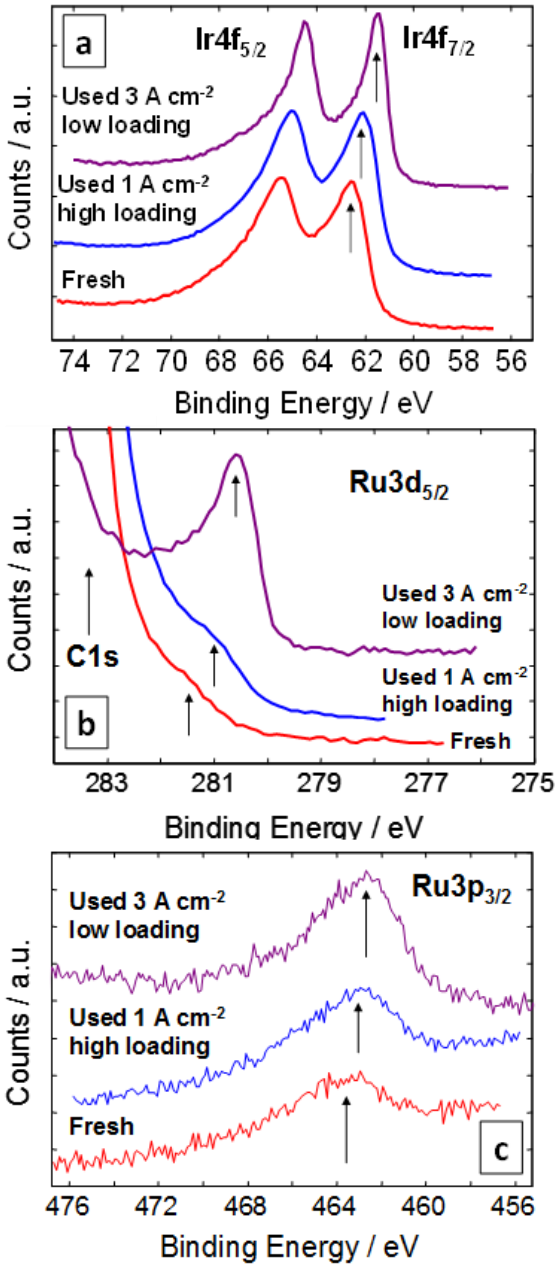

Fig. 14a-c High resolution XP-spectra of the Ir 4f (a), Ru 3d5/2 (b) and Ru 3p3/2 (c) for a fresh electrode, a high loading electrode operated at 1 A cm^{-2} (low turnover frequency) and a low loading electrode operated at 3 A cm^{-2} (high turnover frequency).

A detailed analysis of the Ir 4f region (Fig. 14a) indicates an increasing occurrence of Ir^{3+} species with the increase of operating turn over frequency for the anode. By comparing the B.E. of the Ir4f in the electrodes, the shift to lower B. E. upon operation, in particular at higher turnover frequency, was quite evident (Fig. 14a). Indeed the Ir signal of fresh anode showed a slight shift to higher binding

energy compared to the catalyst powder (Table 1) but this could be caused by interaction with the perfluosulfonic ionomer in the composite catalytic layer after the hot pressing procedure. The Ru3d signal, was especially in the fresh anode and the high catalyst loading electrode, in part masked by the large C1s signal of the ionomer (Fig. 14b). However, a shift of the Ru3d5/2 shoulder appears evident also in this case and a distinct peak is observed for the low catalyst loading anode operated for 1000 hrs at 3 A cm^{-2} (Fig. 14b). This was also corroborated by a similar shift to lower B. E. of the Ru3p3/2 peak (Fig. 14c). Thus, the same phenomena occurring with Ir, are also registered for the Ru sites on the surface producing larger content of Ru^{3+} species. It is derived that a prolonged operation at high turnover frequency causes extraction of oxygen from the Ir-Ru-oxide lattice with the formation of a substoichiometric Ir-Ru oxide phase on the surface.

This causes a modification of the Lewis acidity properties of the catalytic sites producing stronger water chemisorption to saturate defective sites while retarding the rapid release of oxygen molecules during the oxygen evolution process. Formation of substoichiometric Ir species in an oxidative environment is an effect similar to that occurring during high temperature treatment of IrO_2 in air causing decomposition into metallic Ir. Operation at high current density to evolve oxygen at elevated rate may cause, in a similar way, an extraction of oxygen species from the surface.

Table 1. Surface atomic composition and binding energies for a fresh electrode, a high loading electrode operated at 1 A cm^{-2} (low turnover frequency) and a low loading electrode operated at 3 A cm-2 (high turnover frequency).

Sample	Ir +at. %		Ru ++ at. %		Ir 4f B.E. /eV	Ru $3d_{5/2}$ B.E. /eV	Ru $3p_{3/2}$ B.E. /eV	Ir/Ru Atomic Ratio	
	B.S.	A.S.	B.S.	A.S.	B.S.	B.S.	B.S.	B.S.	A.S.
Catalyst powder	79.57	72.3	20.43	27.7	61.95	281.0	463.28	3.89	2.30
Electrode Fresh	79.16	65.50	20.84	34.50	62.52	281.45	463.64	3.80	1.9
Electrode Used 1 A cm^{-2} High Loading	79.09	63.89	20.91	36.11	62.10	280.89	463.06	3.78	1.8
Electrode Used 3 A cm^{-2} Low Loading	69.80	64.95	30.10	35.05	61.49	280.53	462.71	2.31	1.85

+ Determined from Ir4f; ++ determined from Ru3p3/2; *B.S. Before Sputtering; **A.S. After Sputtering

EDX analysis of the low loading MEA operated for 1000 h at 3 A cm^{-2} did not show relevant modification of the bulk composition (~70:30, Ir:Ru at.) after the durability test (not shown). No relevant Ru loss was registered within the experimental error of the EDX technique (not shown). The observed EDX composition, determined at low magnification (150 x) in several regions of the fresh and used MEA was highly constant.

Fig. 15a-c shows TEM micrographs and electron diffraction of different regions of the anodic layer for the low catalyst loading electrode after 1000 h operation at 3 A cm^{-2}. The IrRuOx catalyst appears less agglomerated than in the pristine sample powder, because the perfluorosulfonic ionomer surrounds most of the catalyst agglomerates causing a slight disaggregation of the particles. However, the catalyst morphology appears very similar to the pristine sample showing both faceted and irregular shape particles with average particle size close to the raw sample. All particles appear crystalline and electron diffraction essentially indicate the same crystallographic structure as in the pristine sample

with similar broadening of the diffraction rings. It is difficult from these micrographs to understand if there was an increase of surface roughness after prolonged operation at high current density.

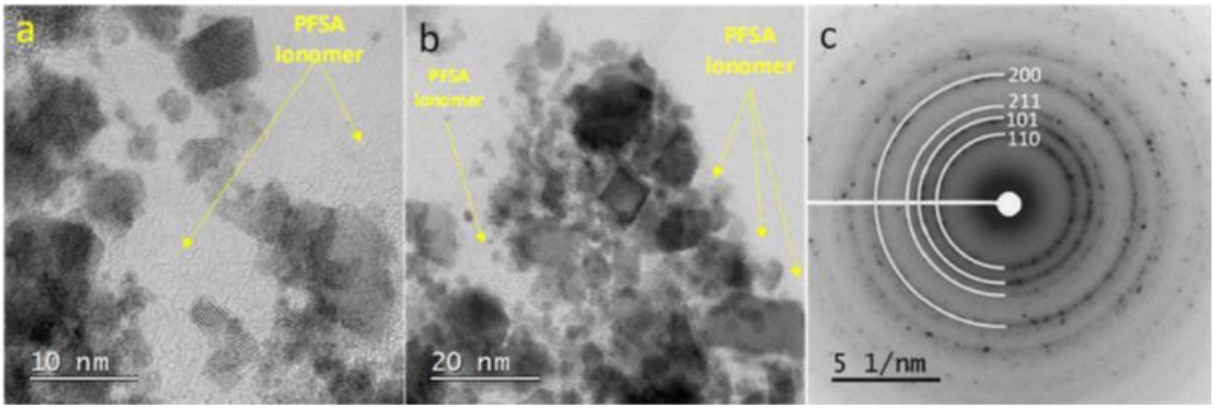

Fig. 15a-c TEM micrographs (a,b) and electron diffraction (b) of different regions of the anodic layer for the low catalyst loading electrode after 1000 h operation at 3 A cm^{-2}.

Also for the low catalyst loading electrode tested for 1000 h at 3 A cm^{-2}, the EDX line scan shows for most of the particles (an example is reported in Fig. 16a-b) an enrichment of Ir on the outer surface, oxygen depletion (sub-stoichiometry) in the outermost layer whereas Ru is mainly located in the particle core. These results are in very good agreement with the XPS analysis.

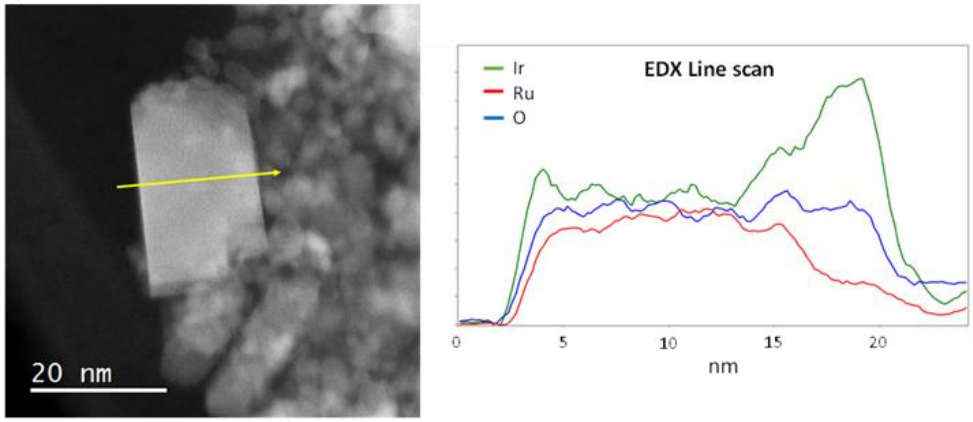

Fig. 16a-b Energy dispersive X-ray analysis (EDX) line scan along an IrRuOx catalyst particle in the low catalyst loading electrode tested for 1000 h at 3 A cm^{-2}

As discussed in the introduction, it is widely reported that the RuO_2 stability is lower than that of IrO_2. However, this is known to be valid for the separate oxides. Whereas, there are not many literature reports giving specific indication of a selective degradation of one of the two components when they are forming a solid solution or the bimetallic system is enriched on the surface with Ir. To get specific insights into the corrosion of the RuO2 and IrO2 forming a solid solution with some segregation of Ir on the surface of the nanoparticles, we have carried out an ex-situ corrosion test in liquid acid electrolyte (as an accelerated stress test) by subjecting the catalyst to step potentials (Fig. 17). In particular, similar potentials of PEM electrolysis experiments were used for the potential steps in half-

cell studies with acidic liquid electrolyte. As mentioned above, the ex-situ measurements represent an accelerated stress test since both the solid polymer electrolyte and the feed of pure water, in PEM electrolysis experiments, mitigate strongly the corrosion with respect to a concentrated liquid acid solution. The corresponding Ir and Ru dissolution was measured by highly sensitive in situ measurements of their respective concentrations using inductively coupled plasma mass spectrometry (ICP-MS). Online time- and potential-resolved electrochemical dissolution profiles revealed interesting corrosion features in the potential window of practical interest (Fig. 17).

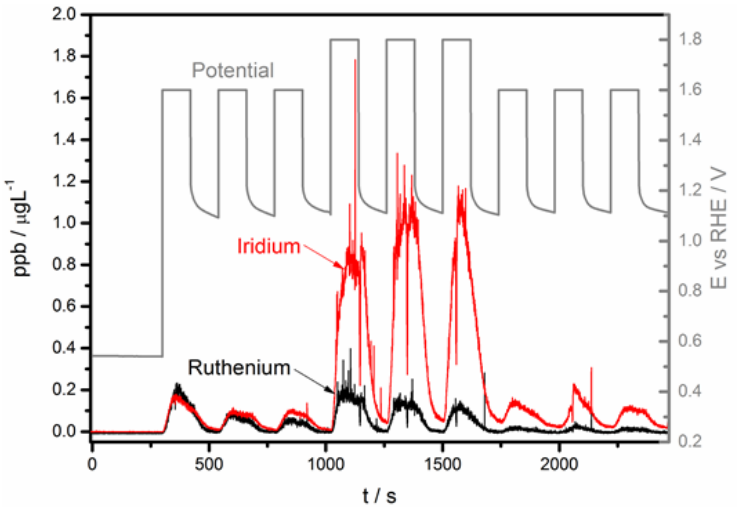

Fig. 17 Electrochemical corrosion test in flow cell coupled with ICP-MS for the pristine Ir-Ru oxide anode catalyst

The electrochemical protocol used in the EFC-ICP-MS experiments was regarding, 5 min operation at the open circuit potential where no dissolution was observed followed by three potential steps to 1.6 V for 2 min each. In the first potential step to 1.6 V RHE, dissolution of Ir and Ru was observed at almost similar extent (Fig. 17). This is somewhat unexpected for a conventional catalyst since RuO_2 is less stable than IrO_2 but it can be explained with the much larger occurrence of Ir atoms in the outermost layers. Thus, the two aspects compensate each other. In the two successive steps at 1.6 V, both the Ir and Ru signals decreased but the concentration of Ru in a significantly larger extent indicating consistent depletion of Ru from the surface (Fig. 17). Thereafter, three potential steps to 1.8 V (2 min each) were carried out. The increase of potential caused strong increase in Ir dissolution (about 4-5 times larger than at 1.6 V) indicating that there is certainly an effect of the potential or the associated increase of reaction rate on the catalyst corrosion. This is in accordance with the mechanism proposed by Kötz where OER proceeds through Ru-oxide and also Ir-oxide as intermediate. Ru dissolution in these three steps at 1.8 V increased less significantly and decreased from the first to the third step (Fig. 17). This may be explained with the minimal content on Ru in the outermost layers. However, it is also considered that, if there is some loss of oxygen from the surface during the electrolysis at high currents, as evidenced by XPS, there may be less chance to form unstable highly oxidized RuO4 species. It could be possible that the increased potential window may extract Ru atoms from the surface underneath layers at least in a first phase of operation. The last three steps from OCP to 1.6 V (2 min each step) show that Ir degradation is returning to the level before the potential steps to 1.8 V whereas Ru dissolution almost disappears a consequence of the Ru depletion from the surface (Fig. 17).

Accordingly, both Ru and Ir dissolution, and modification of the oxidation states can be considered responsible of the anode degradation. The dissolution of Ir and Ru atoms from the outermost layers causes a slight increase of the surface roughness. It is unclear if this may in part compensate for the above degradation phenomena reducing catalytic losses because oxygen evolution is also structure sensitive reaction, requiring neighboring catalytic sites at specific distance to promote bond formation in the oxygen molecule.

3 The Influence of Iridium Chemical Oxidation State on the Performance and Durability of Oxygen Evolution Catalysts in PEM Electrolysis

Nanosized Ir-black (3 nm) and Ir-oxide (5 nm) oxygen evolution electrocatalysts showing high performance in polymer electrolyte membrane (PEM) water electrolysis based on Aquivion ® short-side chain ionomer membrane are investigated to understand the role of the Ir oxidation state on the electrocatalytic activity and stability. Despite the smaller mean crystallite size, the Ir-black electrocatalyst shows significantly lower initial performance than the Ir-oxide. During operation at high current density, the Ir-black shows a decrease of cell potential with time whereas the Ir-oxide catalyst shows increasing cell potential resulting in a degradation rate of about 10 µV/h, approaching 1000 h. The unusual behaviour of the Ir-black results from the oxidation of metallic Ir to IrOx . The Ir-oxide catalyst shows instead a hydrated structure on the surface and a negative shift of about 0.5 eV for the Ir 4f binding energy after 1000 h electrolysis operation. This corresponds to the formation of a sub-stoichiometric Ir-oxide on the surface. These results indicate that a hydrated IrO_2 with high oxidation state on the surface is favourable in decreasing the oxygen evolution overpotential. Modifications of the Ir chemical oxidation state during operation can affect significantly the catalytic activity and durability of the electrolysis system.

3.1 Materials and methods for Ir-metal and Ir-oxide catalysts

Unsupported high surface area IrO_2 was prepared according to a modified Adams fusion method. The thermal activation procedure (500 °C for 10 min) was carried out in a tubular quartz furnace and controlled by using an infrared camera to check for the formation of hot spots. This mild annealing treatment was selected to favour crystallisation while avoiding growth of particle size. After cooling, the unsupported IrO_2 catalyst was washed abundantly with bi-distilled water and pre-leached in 0.1 M perchloric acid at 80°C for 1 h in order to remove eventual impurities from the preparation process.

Iridium black powder was synthesized by chemical reduction of $H_2IrCl_6{\cdot}6H_2O$ using $NaBH_4$ as reducing agent according to D3.1. 40% Pt/Vulcan XC-72 was prepared by the sulphite complex method and used as cathode catalyst in all cases [D3.1]. A 90 µm thick chemical stabilised Aquivion® short-side chain ionomer membrane (E98-09S) with equivalent weight (EW) of 980 g/eq was developed by Solvay Specialty Polymers for water electrolysis applications. Membrane-electrode assemblies (MEAs) were formed by using a catalyst-coated membrane (CCM) preparation procedure. This procedure included initial preparation of separate catalyst slurries of IrO_2 or Ir-black as well as Pt/C with an 830 g/eq equivalent weight-based Aquivion® ionomer dispersion (D83-06A). The Ir-based and Pt-based slurries were sequentially sprayed onto the two opposite faces of an Aquivion membrane to form two types of MEAs one consisting of Ir-black/Aquivion®/Pt and another based on IrO_2/Aquivion®/Pt. The ionomer content in the catalytic layers was 20 and 33 wt. % for the anode and cathode, respectively. CCMs (5 cm^2 geometrical electrode area) were hot-pressed at 190°C, 1.5 min, 20 $kg{\cdot}cm^{-2}$) to favour bonding of the catalytic layers to the membrane at a temperature higher than the glass transition temperature of the ionomer.

The MEA was installed in an electrolysis cell housing equipped with Ti plates. A conventional carbon based gas diffusion layer (GDL ELAT-type) was used for the cathode whereas a Pt-coated titanium fibre mesh (Bekaert Toko Metal Fiber Co.) was used as diffusion layer for the anode. In all experiments, the catalyst loading was fixed at 0.4 mg Ir cm^{-2} for the anode and 0.1 mg Pt cm^{-2} for the cathode. All reported current densities are referred to the geometrical electrode area.

The PEM electrolyser performance was studied at different temperatures and under ambient pressure. Milli-Q Integral, Millipore deionized water characterised by a resistivity of 18.2 MΩ·cm was fed to the anode with a flow rate of 4 mL·min^{-1} and recirculated at the same temperature of the cell. Electrochemical analysis included polarization curves, electrochemical impedance spectroscopy (EIS), cyclic voltammetry and galvanostatic durability tests (1000 h at 1 A cm^{-2}).

These were carried out using an Autolab PGSTAT 302 Potentiostat/Galvanostat equipped with a 20 A booster (Metrohm) and FRA (frequency response analyser). Galvanostatic polarization curves were registered by increasing stepwise the cell current with logarithm increase of current, using a cut-off voltage of 2 V. Electrochemical impedance measurements were carried out at 1.5 V by varying the frequency from 100 kHz to 100 mHz in single sine mode and using a sinusoidal excitation signal of 10 mV. Cyclic voltammetry analysis of the anodic catalyst layer was carried out by feeding hydrogen to the cathode and nitrogen to the anode (driven mode) by using a scan rate of 20 mV·s-1, between 0.4 and 1.4 V RHE. In the CV studies, the cathode was used as both reference and counter electrode whereas the anode was the working electrode.

Chemical and morphological characterizations were carried out on both fresh electrocatalysts and used electrocatalytic layers i.e. before and after a 1000 h durability test. X-ray diffraction (XRD) was performed on the electrocatalysts and catalytic layers by a Philips X-Pert diffractometer using a CuKα as radiation source operating at 40 kV and 20 mA. A scan rate of 0.5° 2θ min -1 with an angular resolution of 0.005° 2θ was used. The diffraction patterns were fitted to the Joint Committee on Powder Diffraction Standards (JCPDS). Scanning Electron Microscopy (SEM) and Energy Dispersive X-Ray (EDX) analysis were carried out by using a FEI XL30 SFEG microscope equipped with EDX spectrometer. The instrument was operated at 25 kV and the EDX probe was used to determine the bulk elemental composition of the anodic electrocatalysts before and after the durability test. The morphology of the electrocatalysts and catalytic layers was investigated by transmission electron microscopy (TEM) using a Philips CM12 instrument. The specimens were prepared by dispersion of the electrocatalyst or electrocatalytic layer powders in isopropyl alcohol and depositing a drop of such suspension on a carbon-coated copper grid. Analysis of surface composition and oxidation states for the Ir-based oxygen evolution electrodes, was carried out by X-ray photoelectron spectroscopy before and after durability tests of 1000 h by using a Physical Electronics (PHI) 5800-01 spectrometer.

3.2 Results and discussion on Ir metal and Ir-oxide catalysts

The aim of this activity was to compare the role of the surface and bulk chemical oxidation state of two iridium catalysts on their performance and stability for operation as oxygen evolution electrocatalyst in PEM water electrolysis. The catalysts preparation procedure was tailored to achieve as much as possible a small mean crystallite size for the unsupported electrocatalysts. All MEAs were equipped with the same cathode electrocatalyst (40% Pt/C) that, according to previous D3.1,

contributes much less in determining the performance and stability of the cell. This is because hydrogen evolution is a relatively fast process compared to the anodic process.

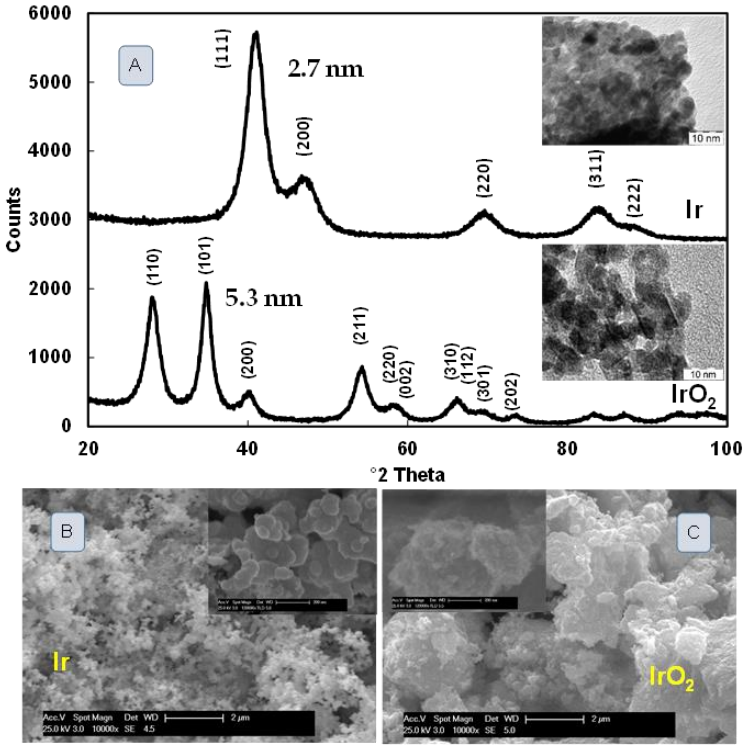

Figure 18. XRD patterns of the Ir (JCPDS card no. 6598) and IrO_2 (JCPDS card no. 15870) catalysts (inset TEM micrographs of Ir and IrO_2) (A); SEM images of Ir (B); SEM images of IrO_2 (C).

Fig. 18a-c provides a picture of structural and morphological properties of the Ir-black and IrO_2 electro-catalysts as provided by XRD, TEM and SEM analyses. The insets in Fig. 18a regard the TEM micrographs of Ir-black and IrO_2 powders. Since these catalysts are unsupported, they appear slightly agglomerated even if characterised by primary particles smaller than 10 nm in both cases. At high magnification, the IrO_2 appears less agglomerated with a significant fraction of pores among the particles. The Ir-black appears more compact but possibly this is due the easier packing of smaller particles. X-ray diffraction patterns (Fig. 18a) showed the presence of a face-centred cubic structure for the Ir-black (JCPDS no. 15870) catalyst and a tetragonal rutile structure for the IrO_2 sample. The mean crystallite size for these samples was determined according to the Debye-Scherrer method by analysing the peak profiles after correction for the instrumental broadening. The (220) reflection in the case of the Ir-black catalyst and the (110) reflection for the IrO_2 were used for this analysis being these peaks less affected by the interference from the other reflections. The mean crystallite size was slightly smaller for the Ir-black (2.7 nm) than in the case of the IrO_2 sample (5.3 nm) accounting for smaller particles.

SEM micrographs obtained at both low magnification (Fig. 18b-c) show a relatively larger porosity for the Ir -black vs IrO_2 whereas at high magnification (Fig. 18b-c insets) the agglomerates of Ir-black were more dense that those of IrO_2 according to the previous evidence from TEM.

In principle, a mean crystallite size of 2.7 nm for Ir-black, as derived from the XRD analysis, should result in a larger number of surface sites than for the Ir-oxide catalyst, which has almost double the

crystallite size, i.e. 5.3 nm. However, the morphologies of these catalysts are different; thus, the smaller mean crystallite size for the Ir-black does not necessarily correspond to a larger number of exposed catalytic sites. Agglomeration effects, which appear more relevant for the Ir-black catalyst, may cause a significant reduction of the available surface sites.

The performance of a PEM electrolyser is generally assessed by carrying out galvanostatic polarisation curves under steady-state conditions (Fig. 19 a-b). The cell potential is measured under steady-state conditions at each applied current density. The oxygen evolution is a temperature activated process showing a decrease of cell potential (increase of efficiency) at the different current densities as the cell temperature increases. The MEAs based on the two different iridium catalysts (Ir-black and Ir-oxide) were compared using the same noble metal loadings (0.4 mg Ir cm^{-2} at the anode and 0.1 mg Pt cm^{-2} at the cathode).

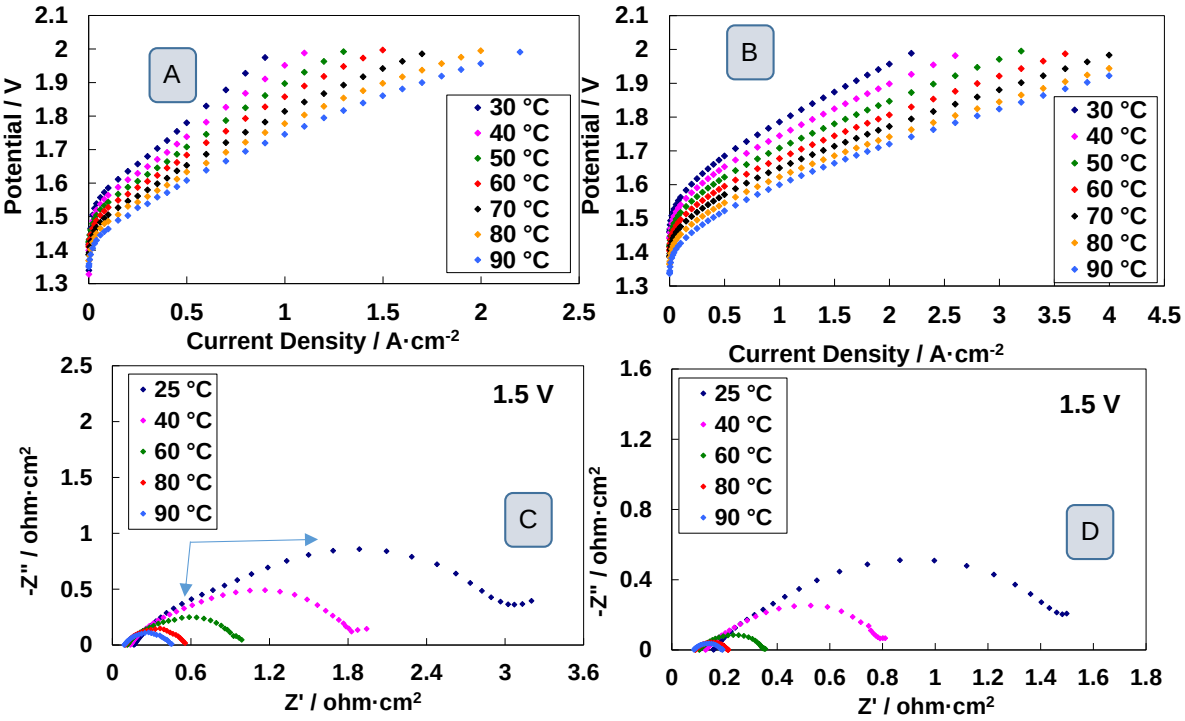

Figure 19. Polarization curves at different temperature (A, B) and Ac-impedance spectra at 1.5 V and different temperature (C, D) of water electrolysis cell with the Ir-black (left) and IrO_2 (right) catalyst- based MEAs.

Interestingly, the Ir-black catalyst shows two curvatures in the polarisation curves especially at high operating temperatures (Fig. 19a). One at low current density (~ 0.1 A cm^{-2}) associated to the electrochemical activation process (Volmer-Butler equation) and another at high current density (about 1 A cm^{-2}) which may be interpreted as due to a change of the electrode characteristics with an improvement of the catalytic properties. Generally, the effects of mass transport tend to worsen at high current densities as well as the ohmic effects. Whereas, the observed improvement in the polarisation trend at high current density and high temperature, corresponding to a slight flattening of the polarisation curve (Fig. 19a) with respect to the usual trend, appears due to a possible surface oxidation of the Ir-black during operation at high oxygen evolution rates. It is pointed out that the

polarisation curves are carried out under pseudo steady-state conditions and the observed phenomenon is associated with an increase of the cell potential with current (Fig. 18a). Contrary to this, the polarisation curves of the Ir-oxide catalyst-based MEA do not show any relevant change in the curve trend (Fig. 19b) with current while showing lower cell potentials at the same current density, thus better efficiencies, compared to the Ir-black based MEA. In the low current density range (up to 100 mA cm^{-2}), Tafel slopes vary from 58 to 75 mV/dec passing from the IrO_2 to Ir-black indicating improved reaction kinetics for the oxide catalyst. At high current density, the Tafel slope of the IrO_2 catalyst increases to 106 mV/dec (not shown) according to a change in the reaction mechanism, e.g. a Temkin-type adsorption isotherm may be prevailing at low current density whereas at high current density the adsorption becomes Langmuir-type. Whereas, for the Ir-black, the Tafel slope increases to 295 mV/dec at high current density (not shown) which suggests the occurrence of some other phenomenon concomitant to the oxygen evolution. Beside the possible effects of larger diffusion limitations for the Ir-black than IrO_2, due a less porous structure, at a nano-scale level, the larger increase in the Tafel slope at high current densities for the Ir-black may, very likely, be related to the concomitant surface modification from metal to oxide as evidenced by the XPS analysis (see below).

Ac-impedance analysis is often used to separate the contribution of the different phenomena influencing the polarisation behaviour. Ac-impedance spectra collected at 1.5 V cell voltage (activation control region) are reported in Fig. 19c and d. The high frequency intercept of the semicircles on the x-axis in the Nyquist plots (Fig. 19c and d) is associated to the ohmic resistance (more precisely reported as series resistance, Rs). The difference between the low frequency intercept in the Nyquist plot and Rs is assumed as the polarisation resistance (Rp). The latter is thus not affected by ohmic features. Rs is similar for both MEAs based on Ir-black and IrO_2 being substantially determined by the membrane properties and it decreases slightly with the temperature in both cases accordingly to the increase of the membrane ionic conductivity. Significant differences are instead observed for the polarisation resistance between the Ir-black and IrO_2. There is a significant contraction of the semicircles with the increase of temperature in both cases, strongly accounting for a temperature activated catalytic process, but the IrO_2 catalyst show substantially lower polarisation resistances than Ir-black in all conditions. These differences are better noted in Fig. 20a and b by comparing polarisation curves and ac-impedance spectra at the same temperature. The polarisation resistance of the Ir-black catalyst is about four times larger than that of IrO_2 under same operating conditions (1.5 V, 80°C). Thus, this clearly indicates that such Ir-oxide is catalytically more active than the investigated Ir-black electrocatalyst.

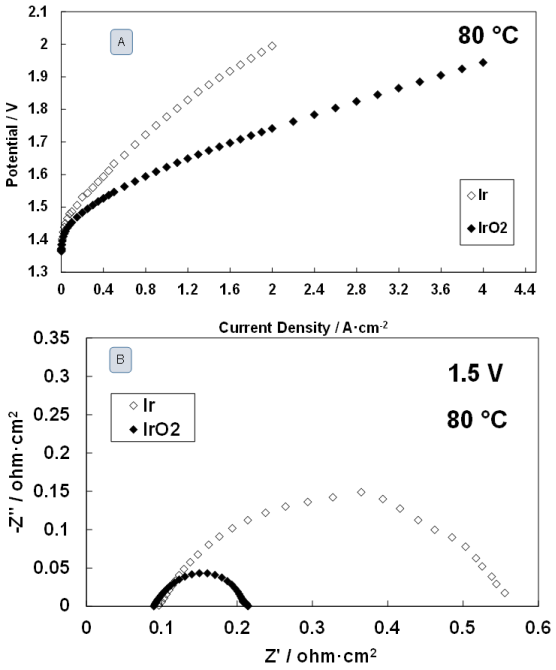

Figure 20. Comparison of polarization curves at 80 °C (A) and Ac-impedance spectra at 1.5 V and 80 °C (B) of water electrolysis cell with the Ir and IrO_2 -based MEAs.

It may be possible that under operation at high current density the surface state of Ir-black modifies becoming more oxidised with a corresponding change in the polarisation curve trend and polarisation resistance. It is assumed that substantial and irreversible surface modifications may require time.

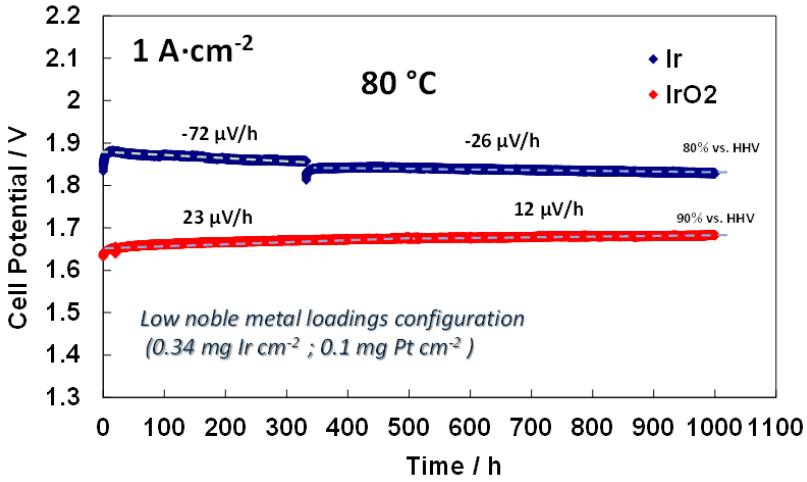

Figure 21. Durability tests at 1 A·cm^{-2} and 80 °C for two different Ir-black and IrO_2 catalysts-based MEAs in the water electrolysis cell.

Accordingly, MEAs based on these electrocatalysts, containing the same noble metal loadings (0.4 mg Ir cm^{-2} at the anode and 0.1 mg Pt cm^{-2} at the cathode), were subjected to durability tests of 1000 each at 1 A cm^{-2} (corresponding to the change of the curvature in the polarisation curve of the Ir- black) and at 80°C (Fig. 21). It is clearly observed that, at the beginning of the durability test, the Ir-black-

based MEA shows a much larger cell potential (1.85-1.9 V) than the IrO_2 catalyst-based MEA (cell potential of 1.65 V). Thus, the two catalysts operate under completely different efficiency regimes with the IrO_2 catalyst being much more efficient in accordance to the polarisation behaviour. However, the cell voltage trend with time is completely opposite for the two catalysts. The Ir-black based MEA shows a fast decrease of cell potential with time corresponding to an increase of efficiency (initial negative trend of -72 µV/h in the first period) especially in the first 200 h. The curve tends to flatten showing a lower negative trend of -26 µV/h in the latter operating period approaching 1000 h duration. On the contrary, the IrO_2 shows an increase of cell voltage with time corresponding to a degradation rate of about 12 µV/h in the last period.

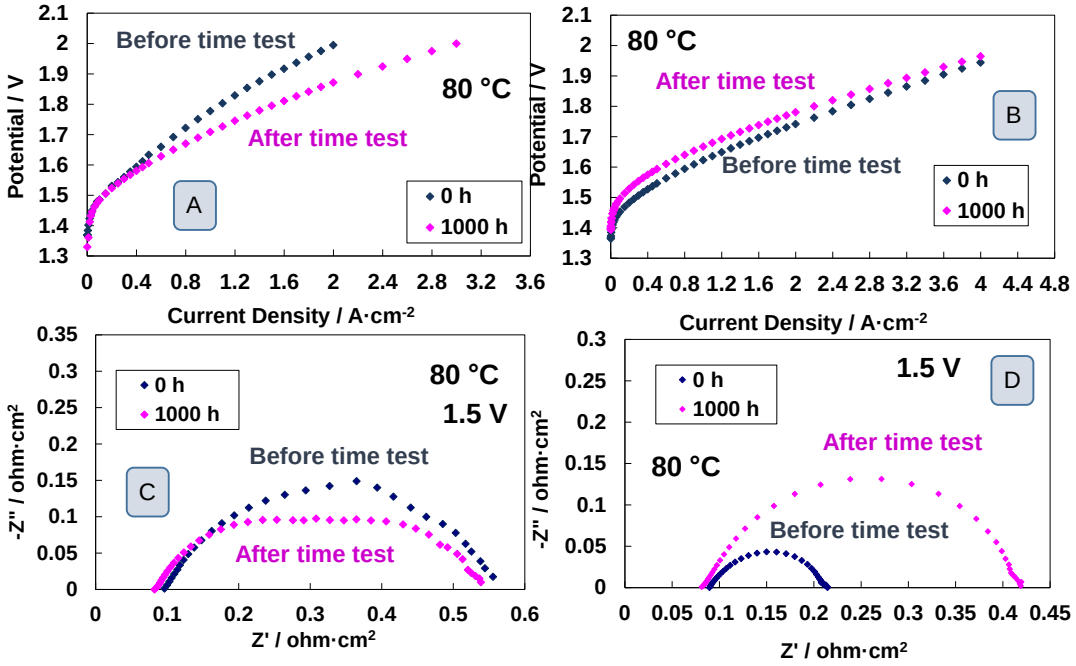

Figure 22. Polarization curves at 80 °C (A, B) and Ac-impedance spectra at 80 °C and 1.5 V (C, D) before and after the 1000 h durability test for water electrolysis cell based on the Ir-black (left) and IrO_2 (right) electrocatalysts.

One may expect that the Ir-black based MEA can approach, after prolonged operation, the efficiency of the IrO_2. However, it is not sure that this may happen since these endurance curves usually tend to flatten after prolonged periods of operation (e.g. after a few thousands hours). It is hypothesized that the Ir-black, after having reached a steady-state condition about its surface chemistry, may invert the trend of cell voltage with time eventually showing a degradation rate trend similar to IrO_2. This possible evolution of the electrolysis behaviour with time for the two catalysts was not studied because, according to the observed trend of voltage variation with time in the last period of our endurance tests, the intersection of the two curves should occur after about 8000 h (about 1 year). This is extrapolated assuming that the trends remain the same also during prolonged operation; however, some literature reports suggest that a flattening of the PEM electrolysis durability curves occurs for several Ir-catalysts based MEAs after several thousand hours of operation. Assuming that the Ir-black catalyst may reach after one or two years of operation the performance of the IrO_2 catalyst, it is clear that it has operated for this large period of time with a

voltage efficiency or enthalpy efficiency at least 10% lower, i.e. 80 vs 90% (calculated on the basis of the thermoneutral potential of 1.47 V at 80°C).

A typical stack duration in some PEM electrolysis applications is about 40000 h corresponding to about 4.5 years. Depending on the effective cost of electricity used in the specific electrolysis applications, one year of operation at about 10 % lower voltage efficiency may be relevant. Another interesting feature is regarding the rapid raise of potential vs time in the first hours at the beginning of the electrolysis experiments. This is usually associated to the reversible losses caused by mass transport constraints e.g. supersaturation of the catalytic layer with the evolved gas at high current density. This phenomenon, although accounts for a limited loss of potential, is more pronounced for the Ir-black catalyst especially at the beginning of the durability test. As discussed above, the less porous structure at a nano-scale level of the Ir-black may result in increased mass transport limitations compared to the Ir-oxide. A successive interruption of the test operation of the Ir-black for one day after about 350 h resulted in slightly lower increase of recoverable losses.

In order to better understand the modifications occurring after the durability tests, the two MEAs were subjected to electrochemical diagnostics (polarisation and ac-impedance after the 1000 hrs endurance tests) and the results compared to the initial behaviour. It is interesting to note that the Ir-black based MEA substantially improved its performance after 1000 h operation at 1 A cm^{-2} (Fig. 22a) even if this remained relatively poor compared to the IrO_2 catalyst (compare Fig. 22a and Fig 22b). Moreover, the second curvature in the polarisation curve of the Ir-black almost disappeared after 1000 h ((Fig. 22a) showing a polarisation profile very similar to that of IrO_2 (Fig 22b).

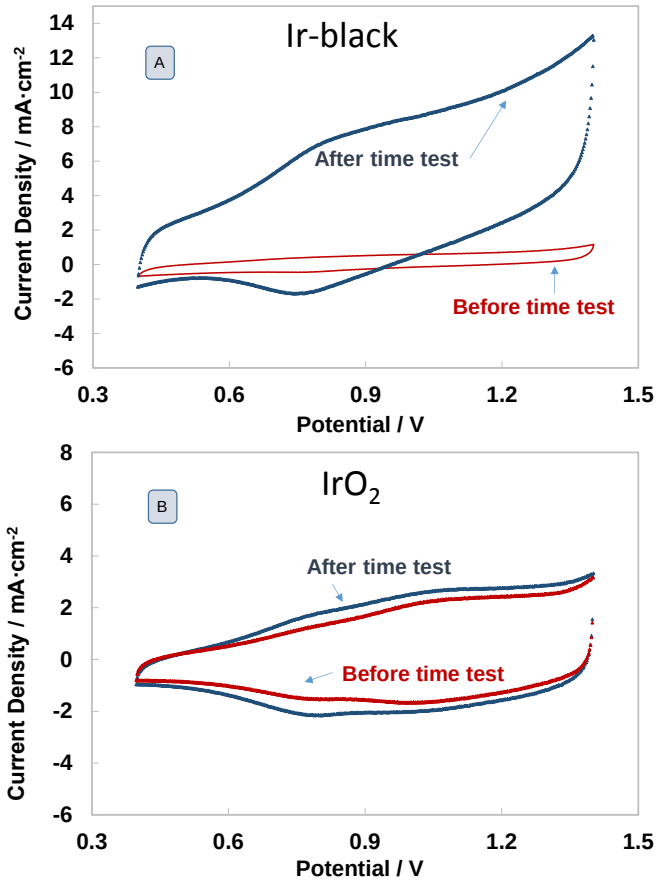

Figure 23. Cyclic voltammetry analysis of the Ir (A) and IrO_2 (B) anode electrocatalyst in the fresh and used (1 A cm^{-2}, 1000 h) MEAs

Ac impedance spectra showed a decrease of polarisation resistance for the Ir-black after 1000 h electrolysis test. Two overlapping semicircles are envisaged in the Nyquist plot of the Ir-black based MEA after the 1000 h electrolysis test as compared to the single semicircle before operation. One may envisage that the additional semicircle appearing at higher frequency is possibly associated to the presence of an additional catalytic phase showing faster relaxation times for the charge transfer in the electrolysis process. On the contrary, the ac-impedance spectra of the IrO_2 based MEA show a slight increase of polarisation resistance after the prolonged operation. A decrease of the value of the imaginary component (Z") of the impedance vector after 1000 h test, may indicate an increase of the double layer capacitance. This was verified by carrying out cyclic voltammetry analysis in the range 0.4-1.4 V RHE (Fig. 23 a). It was observed a relevant increase of the double layer capacitance for the Ir-black after the time test. This relevant change can not be associated to a decrease of the mean particle size but more likely to a change of the chemical properties as a consequence of the possible surface modification of the metallic Ir into an oxide which is usually characterised by much larger capacitance (Fig. 23 a). In comparison, the Ir-oxide catalyst shows just a modest increase of double-layer capacitance after 1000 h operation indicating no substantial changes, possibly a moderate increase of surface roughness due to the electrolysis operation at high current density (Fig. 23 b).

Ac-impedance spectra show that that there is no increase of series resistance that may be associated to the degradation of the Pt-coated Ti diffusion layer, e.g. passivation of titanium, or increase of membrane resistance after the durability tests. Possibly, the cathode catalyst ageing may contribute to the measured degradation rate of the IrO_2 -based cell; however, this should occur only in a very small extent being this process relatively fast and, thus, not contributing significantly to the polarisation resistance. Hydrogen evolution usually affects the high frequency region of the arcs in the Nyquist plots whereas the ac-impedance spectra of the IrO_2 -based catalyst show an increase of the polarisation resistance with time especially at low frequency, in the relaxation time region that is typically related to the oxygen evolution process.

The voltammetric charge of the raw Ir-black catalyst appears significantly lower than that of the Ir-oxide system. Accordingly, one would consider that the significantly lower activity of the Ir-black compared to the Ir-oxide is just related to the lower electrochemically active surface area (ECSA). However, the nature and stoichiometry of surface reactions, occurring during the cyclic voltammetry measurements, for these different Ir-based catalytic systems (metal and oxide), are not known precisely. Usually, the voltammetric charge, obtained from cyclic voltammetry curves, represents a measure of the number of surface active sites, or the electrochemically active surface area, specifically in the case of oxide surfaces. But, for completely different electrode surfaces (metallic and oxidised), the CV measurements may not provide a quantitative comparison of the number of catalytic sites. An oxide material is usually characterised by much larger capacitance values than a corresponding metal of similar surface area. As an example, a hydrous oxide layer, grown on iridium metal under potential cycling conditions, causes, after just a few cycles, a dramatic increase of the voltammetric charge.

After 1000 h operation at 1 A cm^{-2}, the voltammetric charge of the Ir-black system increases significantly. This may suggest essentially two phenomena: a dramatic increase of surface roughness, possibly related to dissolution of the outermost surface layers, and/or the formation of an

oxidised surface (as clearly identified by the XPS analysis below). The latter should also produce a consequent increase of the capacitance, as one would expect because of the change of the nature of the surface from metal to oxide. In particular, after prolonged operation, the Ir-black system largely surpasses in terms of voltammetric charge the fresh and used (1000 h) IrO_2 -based samples. This may occur simply because the crystallite size (average volume diameter of the particles from XRD analysis) of the Ir-black is smaller. Thus, from simple geometric considerations, once the Ir-black material is oxidised on the surface, the effective number of surface sites, should be, in principle, larger than the Ir-oxide catalyst.

To better understand such evidences and to investigate if structural and chemical modifications have occurred for the electrocatalysts after 1000 h electrolysis operation at 1 A cm^{-2}, the MEAs were analysed by X-ray diffraction, X-ray photoelectron spectroscopy and finally by energy dispersive X-ray analysis and transmission electron microscopy. The anode electrocatalysts did not show any alteration of its bulk structure after the durability test and no relevant change of the crystallite size (Fig. 24 a-b).

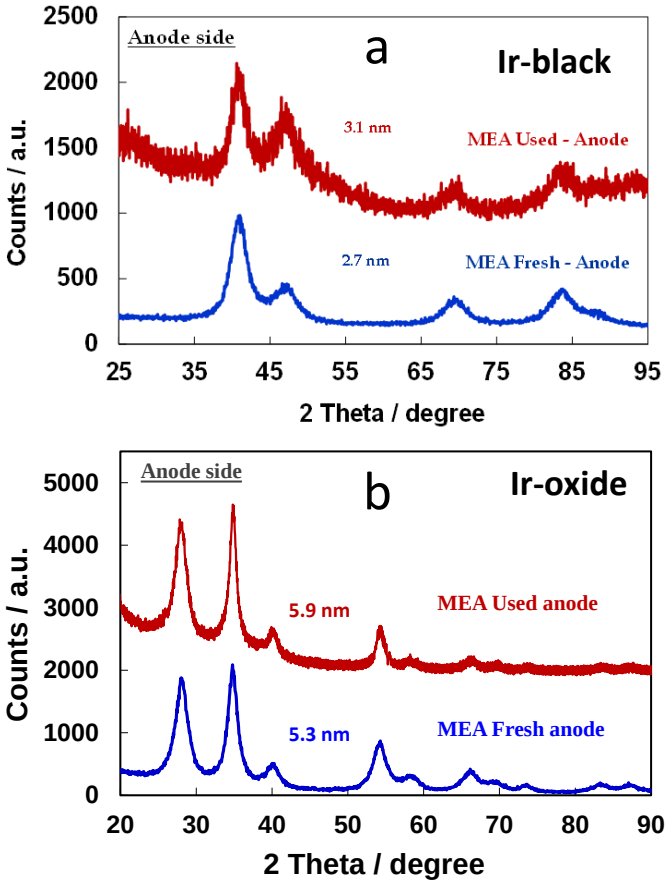

Figure 24 a-b. XRD patterns of the Ir black (a) and IrO_2 (b) anodes in the fresh and used (1 A cm^{-2}, 1000 h) MEAs.

Fig. 24 a shows the case of the Ir-black electrocatalyst with a moderate increase of the crystallite size from 2.7 to 3.1 nm. Similar evidences were observed for the IrO_2 catalyst with a slight increase of the crystallite size from 5.3 to 5.9 nm after operation (Fig. 24 b). Thus, the structural properties were substantially unaffected as well as the crystallite size. Regarding the bulk, both catalysts remained

essentially the same i.e. Ir-black (metallic fcc cubic structure with zero-valent state) and IrO_2 (oxidised, 4+, tetragonal rutile type structure), after the 1000 h electrolysis operation according to the XRD analysis. XPS survey spectra of the Ir-black catalyst before and after testing for 1000 h showed a substantial increase of the O1s signal after operation (not shown). This increase was not so significant in the case of the IrO_2 catalytic layer. Thus, the increase of oxygen content can not be entirely related to the uptake of adventitious species but should be mainly due to the oxidation of Ir on the surface. Interestingly, there was a modification of the fluorine signal. The survey spectra clearly show a decrease of the F KLL Auger lines associated to fluorine. This can be due to a reorientation or restructuring of the ionomer side chains vs. the backbone chain of the ionomer around the catalyst agglomerates.

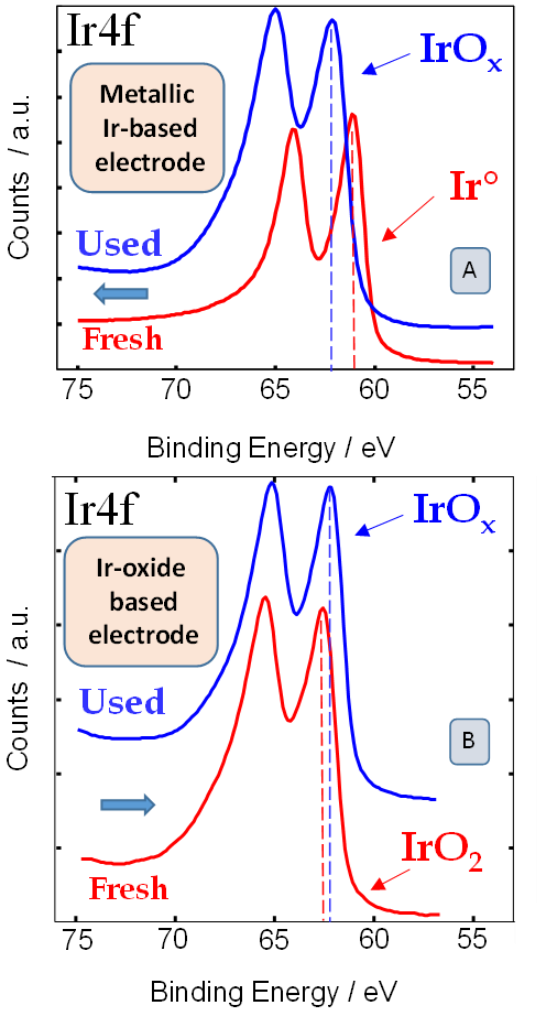

Figure 25. High resolution XPS spectra for Ir signal in the fresh and used (1 A cm^{-2}, 1000 h) anode electrodes for Ir (A) and IrO_2 (B) based electrode

High resolution XPS spectra of the Ir-black based catalytic layer showed a significant shift of the Ir 4f doublet to higher binding energies (Ir4f 7/2 from 61.2 to 62.2 eV) (Fig 25a). This huge shift is clearly associated to the formation of IrOx species on the surface with Ir present mainly in the 3+/4+ oxidation state comparable to a substoichiometric Ir-oxide material. However, the increased broadening of the Ir 4f doublet after the durability test (Fig 25a) may indicate the presence of several oxidations states

including the metallic state. Thus, this conversion may not be complete after 1000 h. Interestingly, also the Ir 4f signal in the IrO_2 -based MEA showed a shift of its binding energies but this was in the opposite direction, i.e. to lower binding energy (from 62.5 to 62.2 eV), accounting for the formation of a sub-stoichiometric Ir-oxide (Fig 25b). Also in this case, some increase in the broadening of the Ir 4f peak (Fig 25b) would indicate that more than one species is present on the surface and just a partial conversion of IrO_2 to IrOx occurs .

A pure rutile structure on the surface is generally characterised by an Ir4f 7/2 peak at 61.8 eV, while the Ir4f 7/2 peak at 62.5 eV, observed in the Ir-oxide sample before the endurance test, would instead indicate the presence of a hydrated structure on the surface, e.g. $IrO_2 \cdot (H_2O)x$. This hydrated IrO_2 structure is very likely formed on the surface as a consequence of the mild annealing process (500 °C for 10 min). This thermal annealing is less strong compared to a treatment at 600 °C for 5 h to achieve the rutile IrO_2 phase on the surface (B.E. of about 61.6 eV). Whereas, the present Ir-oxide sample treated at 500 °C consists of the rutile IrO_2 phase in the bulk according to the XRD analysis. The mild annealing process for the Ir-oxide sample is designed to avoid excessive growth of the catalyst particles while favouring proper crystallisation in the bulk. Interestingly, despite the larger capacitance achieved by the Ir-black after its conversion to IrOx and the similar B.E. for the Ir4f 7/2 of the anodes subjected to the endurance tests, the performance of the Ir-black electrode did not approach that of the Ir oxide-based sample after 1000 h. This is possibly because the interconversion from metal to oxide was not yet complete and some Ir-metal sites were still present on the surface or there was a relevant electronic effect from the Ir-metal core (Fig. 24). This may be expected considering that the primary particles or the crystallites in the case of the Ir-black (according to the XRD analysis) have remained 2-3 nm in size after the durability test at 1000 h at 1 A cm^{-2}. A reduced asymmetry in the Ir7f spectrum of the used Ir-oxide sample and a slight shift towards higher B.E. values would indicate a less metallic character than the used Ir-black; yet, such differences appear not so relevant. Instead, the O1s spectra of the anodes, after the endurance tests, show completely different characteristics (Fig. 26) revealing a different arrangement of the oxygen species on the surface.

Fig. 26 shows the variation of the O1s peak for the Ir-black based catalytic layer after the durability test. The fresh Ir-black catalytic layer shows a shoulder in the O1s spectrum at high B.E. values (534.5 eV) accounting for some adventitious oxygen from the preparation procedure or some organic oxygen from the ionomer and a main peak at 531.5 eV associated to a transition metal oxide. The latter increased significantly in intensity after operation clearly showing the formation of IrOx on the surface of the Ir-black catalyst. The O1s spectra of the Ir oxide-based anode does not show any appearance of the lattice oxygen at 530 eV usually assigned to the rutile structure. Instead, hydroxyl groups at around 532 eV are largely prevailing for both fresh and used Ir-oxide electrocatalysts (Fig. 26) accounting for a highly hydrated surface. In particular, the O1s peak negatively shifts from 532.3 to 532.0 eV after 1000 h operation at 1 A cm^{-2} (Fig. 26). As a comparison, the used Ir-black electrocatalyst shows the main O1s peak at 531.2 eV indicating a less hydrated surface oxide with a shoulder at about 530 eV generally associated to a rutile phase. Accordingly, the main difference in the surface properties of the used Ir-Black and Ir-oxide catalysts appear to rely on the degree of hydration or the content of hydroxyl groups on the surface. A positive influence of weakly bonded surface hydroxyls in Ir-based electrocatalysts on the specific activity for the oxygen evolution process

has been observed in the literature. In particular, surface OH groups have been assumed to act as reactive surface intermediates on active sites of the oxygen evolution process.

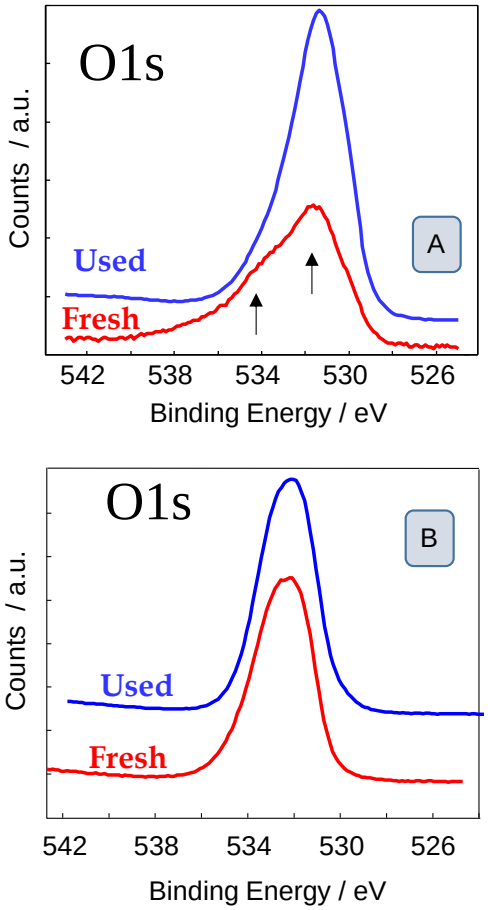

Figure 26. High resolution XPS spectra for O signal in the fresh and used (1 A cm^{-2}, 1000 h) anode electrodes for Ir-black (A) and IrO_2 (B) based electrode

An increase of the oxygen content for the used Ir-black based catalyst compared to the fresh sample was also corroborated by EDX analysis (Fig. 27) indicating that possibly, this modification is not just involving a few atomic layers on the surface but is progressing towards the bulk. However, the increased oxygen content does not reach the level of that in the IrO_2 catalyst (Fig. 27). The bulk of this catalyst remains metallic after 1000 h according to the XRD results but its progressive modification appears to be just matter of time.

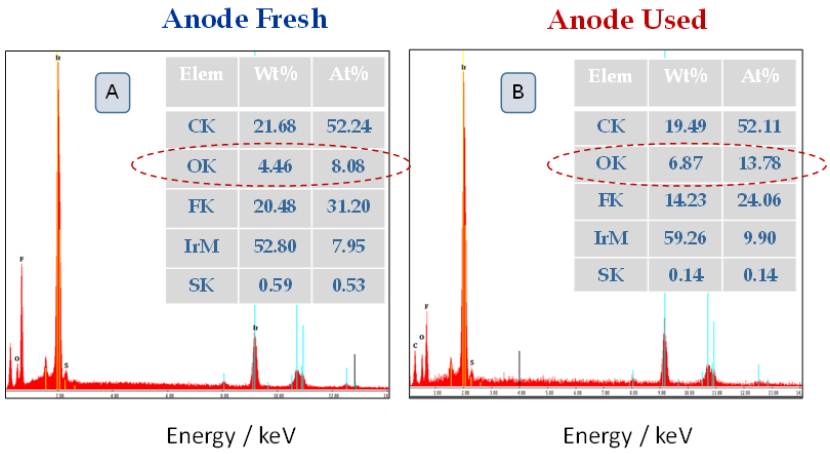

Figure 27. SEM-EDX analysis of the fresh (A) and used (B) (1 A cm^{-2}, 1000 h) Ir anode electrodes

TEM analysis of the Ir-black–based catalytic layer (Fig. 28a-b) suggests that the Ir clusters are initially embedded into the ionomer layer but these partially disaggregate after operation as consequence of the oxygen evolution from the inner particles in the agglomerate or by effect of the infiltration of the ionomer inside the catalyst agglomerates. Similar evidence was observed for the IrO_2-based catalytic layer (Fig. 28c-d) but no increase of the particle size was envisaged in both cases.

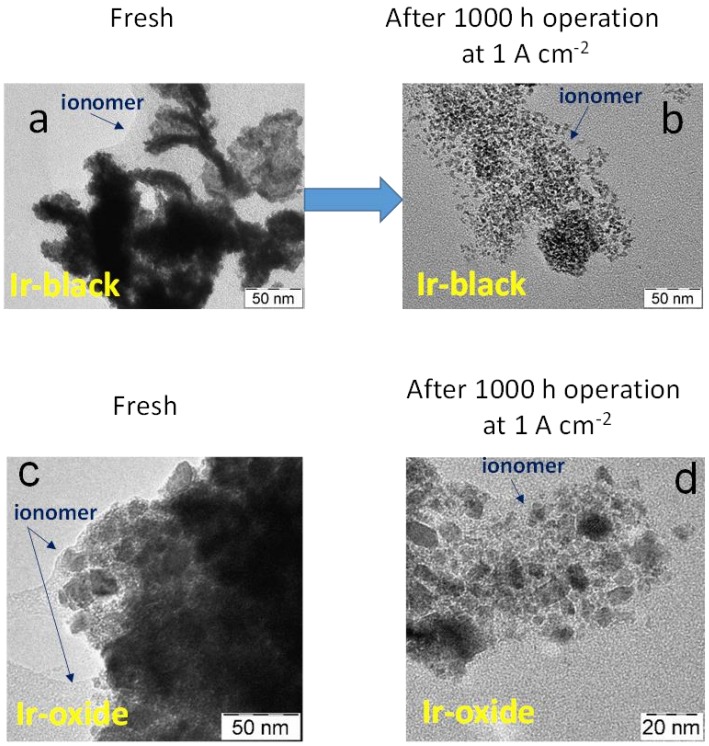

Figure 28. TEM micrographs of the fresh (a) and used (b) catalytic layers based on the Ir black anode catalyst. TEM micrographs of the fresh (c) and used (d) catalytic layers based on the Ir-oxide anode catalyst.

Oxidation of the metallic Ir surface during the oxygen evolution process is clearly justified by its reaction with water at high operating potentials, according to the Pourbaix diagram. This transformation process is kinetically controlled and, possibly, it requires time to reach completeness. Less expected is the formation of sub-stoichiometric Ir-oxide during operation of the IrO_2 catalyst. This process corresponds to a partial change from an Ir (IV) oxidation state to an Ir (III) state. Accordingly, the ageing of the Ir-oxide catalyst appears essentially related to the oxygen evolution in acidic environment, which possibly leads to amorphisation on the surface and formation of Ir (III) species. Moreover, a decrease of the content of hydroxyl groups on the surface with time may produce a decay in performance. In principle, the presence of the perfluorinated ionomer around the catalyst (TEM images show in several cases that the catalyst clusters are embedded by the ionomer layer) favours, through its interaction with the catalyst surface, the occurrence of fully oxidised Ir sites on the surface. As speculative hypothesis, a possible rearrangement of the perfluorinated ionomer around catalyst clusters during electrolysis operation, as envisaged from a decrease of the intensity of the fluorine signal in the XPS spectra, may occur with time. This could be possibly related to the disaggregation of the catalyst clusters from the ionomer as consequence of the oxygen evolution at high reaction rates, as observed from TEM analysis (Fig. 28). Such phenomenon may contribute in producing a modification of the Ir sites chemistry. However, an in depth analysis is needed to corroborate this speculative hypothesis and this will be the object of successive work. An interaction of the iridium sites with the perfluorinated ionomer can make them more electrophilic because of the electron withdrawing effect of fluorine. Another possible cause of the Ir 4f shift to lower B.E. with time may arise from the fact that the oxygen evolution process can involve the lattice oxygen producing some surface modification especially when the process occurs at high reaction rates. From the observed results, it appears clear that an iridium oxide, obtained from a mild annealing process and characterised by a large content of hydroxyl groups on the surface, is significantly more active than an iridium black catalyst for the oxygen evolution process. Moreover, poorly hydrated sub-stoichiometric IrOx species show intermediate operating potential between largely hydrated Ir-oxide and metallic Ir. Higher activity of hydrated structures has been numerously reported in this field. The oxygen evolution process can proceed at high rates especially in the presence of surface intermediates, such as OH groups, displaying a balanced binding to the oxide lattice. In particular, surface OH groups, loosely bound to the oxide lattice, can promote the oxygen evolution process. Although the surface hydroxyl groups display nominally higher XPS binding energies than the lattice oxygen, e.g. bridged lattice oxygen or terminal oxygen groups which are bound strongly, the chemical bond strength of the OH groups varies with local coordination.

In the present activity, we have observed that the performance degradation with time for the hydrated IrO_2 corresponds to a negative shift of the B.E. of Ir 4f indicating that the Ir sites became less electrophilic during operation. Accordingly, they become characterised by a lower capability to adsorb oxygen species as intermediate reaction step of the oxygen evolution process that precedes the O-O bond formation. In other words, this corresponds essentially to a decrease of the Lewis acidity of Ir cations in the oxide. Such aspect plays a paramount role in promoting the interaction with water molecules in hydroxylated surfaces and the transfer of protons from the adsorbed water molecules to the neighbouring lattice oxygen sites to give rise to water dissociation.

4 Conclusions

This deliverable addresses the development of advanced oxygen evolution reaction catalysts for PEM electrolysis applications. Particular efforts were addressed to put in evidence a good correlation between PEM electrolysis degradation results and the ex-situ catalyst corrosion in liquid electrolyte. In particular, the cell with larger catalyst loading operating at 1 A cm^{-2} (about 1.6 V of cell voltage) shows degradation rate of 5 µV/h whereas the one operating at 3 A cm^{-2} (about 1.8 V of cell voltage) shows degradation rate of 15 µV/h corresponding to a three times increase of corrosion rate. Similar trend is observed for the low catalyst loading MEA even if the level of corrosion at both current loads is higher when turnover frequency increases. These results are in line with the data obtained from EFC-ICP-MS tests, showing a significant increase of dissolution rate when the catalyst is operated at higher potentials corresponding to higher reaction rate. Moreover, it is clear from EFC-ICP-MS that dissolution is affecting both metals (not just Ru). In particular, after a first removal of a small content of unstable Ru atoms present on the surface, the dissolution rate is essentially corresponding to the surface occurrence of the two metals as determined by XPS. This represents an erosion of the catalyst nanoparticles. In principle, the increased surface roughness may compensate in terms of surface area with respect to the catalytic losses caused by dissolution of surface layers; thus, it seems there is no much effect on the electrochemical surface area. This appears to slightly increase in the first 1000 h due to the increase of the surface roughness as a consequence of the erosion of the outermost catalyst layers. The fact that Ru dissolution is getting lower with time in half-cell tests is clearly explained with the evidence that Ru atoms are concentrated in the bulk of these nanoparticles. Thus, corrosion is necessarily affecting in a larger extent the element that is occurring more frequently on the surface i.e. Ir. By comparing the information from electron microscopy and XPS, it was evident that there is a specific segregation of Ir atoms on the catalyst surface. Although the catalyst is characterized by good crystallinity, there are so many small crystalline domains (3 nm) or irregular particles characterized by large amount of defects and showing different crystal orientations. It is possible that these particles are primarily affected by corrosion and degradation phenomena than large particles which appear almost free of defects. This can also explain why the largest performance loss in PEM electrolysis occurs indeed within the first hours of operation where unstable particles may rearrange to form more stable crystalline domains but possibly characterized by lower intrinsic activity. Of course, a larger heat release from the reaction process during operation at high turn-over frequencies can speed-up the transformation of small unstable nanoparticles. Thus, a rapid loss or modification of specific catalytic sites occurs compared to the operation with a low turnover frequency. A correlation between degradation rate in PEM electrolysis and turn-over frequency as well as thermal power production per catalytic site is envisaged. This effect appears prevailing with respect to the operating potential window. Moreover, as evidenced by XPS, catalyst operation at high turnover frequency causes a progressive change with time of Lewis acidity characteristics of the Ir and Ru cations thus influencing their ability to promote water chemisorption and dissociation on the anode surface being this the rate determining step of the overall process.

This deliverable provides, also, evidence of a correlation between the PEM electrolysis behaviour (performance and cell voltage variation with time) and the chemical oxidation state of Ir in the oxygen evolution catalyst (responsible for the rate determining process). In particular, during operation at 1 A cm^{-2}, the cell with Ir-black (metallic Ir) catalyst (characterized by an initial cell voltage about 1.9

V) shows a negative variation of potential with time. On the contrary, the cell containing the high surface area IrO_2 (Ir4+) catalyst (about 1.65 V cell voltage) shows a degradation rate of about 10 µV/h (voltage increase with time) while approaching the 1000 h of operation. The voltage variation appears to flatten with time in both cases but the IrO_2 catalyst operates at about 90% voltage efficiency (enthalpy efficiency) compared to about 80% for the metallic Ir. Both catalysts experience modifications during 1000 h operation. An increase of voltammetric charge with time is recorded in both cases (more significant for the Ir-black). Surface oxidation of the metallic Ir to IrOx and partial reduction of the IrO_2 catalyst, highly hydrated on the surface, to form a substoichiometric surface oxide (Ir3+/Ir4+) occur during operation. The latter phenomenon may be also favoured by a rearrangement of the perfluorinated ionomer around the catalyst agglomerates as envisaged from TEM analysis. This may affect the oxidation state on the surface since fluorine species produce an electron withdrawing effect making the Ir sites more oxidized. Thus, during operation at 1 A cm^{-2}, the modifications of the Ir-black catalyst produce a continuous improvement in efficiency whereas the efficiency decreases with time for the IrO_2 catalyst-based cell. Probably, these effects are exacerbated during the first thousand hours of operation and will mitigate with time or a modification of the observed trends may occur after several thousand hours.

The results appear to indicate that a high oxidation state for Ir along with a hydroxylated surface can reduce the overpotential of the oxygen evolution process at a specific current density. This is in agreement with several reported evidences in the literature showing higher activity for the oxygen evolution of hydrated Ir-oxide structures. A catalyst made of metallic Ir in the core (bulk) and IrOx on the surface appears to perform better than the initial Ir-black (metallic Ir both on the surface and in the bulk of the catalyst). However, this configuration seems less active than the combination of oxidized IrO_2 that is hydroxylated on the surface while consisting of IrO_2 rutile structure in the bulk. This situation may be eventually influenced by the presence of residual metallic Ir on the surface of the Ir-black after operation and it should be confirmed for the case of a full oxidation of the outermost layers. Changes of the Ir chemical oxidation state on the surface during operation are thus of paramount importance and affect performance and durability of the electrolysis system.

5 Acknowledgements

The authors thank the Fuel Cells and Hydrogen 2 Joint Undertaking (FCH JU) for the financial support through the HPEM2GAS project. This project has received funding from the Fuel Cells and Hydrogen 2 Joint Undertaking under grant agreement No 700008. This Joint Undertaking receives support from the European Union's Horizon 2020 research and innovation programme, and Hydrogen Europe (Industry grouping), and Hydrogen Europe Research (Research grouping).

Some activities here reported were carried out in collaboration with the National Institute of Chemistry, Ljubljana, Slovenia (N. Hodnik, P. Jovanovic, F. Ruiz-Zepeda, M. Šala), the National Research University "Moscow Power Engineering Institute", Moscow, Russia (S.A. Grigoriev) and the National Research Centre "Kurchatov Institute", Kurchatov Moscow, Russia (V.N. Fateev). We thank these colleagues for their contribution.